Construction and Building Materials

Effect of Graphene Oxide Nanoparticles on Blast Load Resistance of Steel Fiber Reinforced Concrete

--Manuscript Draft--

Manuscript Number:	CONBUILDMAT-D-22-03838R1
Article Type:	Research Paper
Keywords:	Graphene oxide; Steel fiber; Fiber reinforced mortar; Blast resistance; Blast loading; TNT; Non-contact detonation
Corresponding Author:	Buchit Maho, Ph.D. Rajamangala University of Technology Phra Nakhon Dusit, Bangkok THAILAND
First Author:	Sittisak Jamnam
Order of Authors:	Sittisak Jamnam
	Buchit Maho, Ph.D.
	Apisit Techaphatthanakon
	Chesta Ruttanapun
	Peerasak Aemlaor
	Hexin Zhang
	Piti Sukontasukkul
Abstract:	Concrete structures may occasionally be subjected to both intentional or unintentional explosions which could cause casualties and damage to properties. Advance research on protective structures are important to enhance blast resistance of materials, and to protect life and properties. This study investigated the effect of graphene oxide nanoparticles (GO) on enhancing the blast resistance of fiber reinforced cement mortar (FRM). GO in solution was incorporated in steel fiber reinforced mortar at the rate of 0, 0.025, 0.050, 0.075, and 0.100% by weight of cement. A series of experiments were carried out consisting of 2 stages: Stage 1) workability, setting time, compressive and flexural strength, and microstructure using SEM and XRD processes, and Stage 2) blasting loading test. The optimum GO dosage giving the highest compressive and flexural strengths from the 1 st stage was determined and chosen to continue on the 2 nd stage (blast loading test). The blasting tests were performed on panel specimens (500mmx1000mmx60mm) using TNT weighing ½ lb. (226.7 grams) with three different standoff distances of 340, 400, and 460 mm. Results from Stage 1 on both flexural and compression tests indicated an optimum GO content of 0.025% by weight of cement. The workability was found to decrease with the increasing the GO content. The SEM images also revealed that the addition of GO nanoparticles reduced the porosity in the mortar matrix. For the blasting test, three damage patterns were observed: complete flexural failure, partial damage (flexural cracking), and no major damage, depending on the standoff distance and specimen type. The addition of GO can reduce the maximum and permanent deflections of the panel under blast loading. FRM panels with GO at 0.025% tested at the standoff distance of 460 mm showed the lowest level of damage.
Suggested Reviewers:	Banthia Nemkumar, Professor The University of British Columbia banthia@civil.ubc.ca Specialist on impact loading in concrete
	Eiki Yamaguchi, Professor Kyushu Institute of Technology: Kyushu Kogyo Daigaku yamaguch@civil.kyutech.ac.jp A specialist on structure
	Fujikake Kazunori, Professor National Defense Academy of Japan fujikake@nda.ac.jp

Powered by Editorial Manager® and ProduXion Manager® from Aries Systems Corporation

	A specialist on impact loading in structure
	Sonoda Yoshimi, Professor Kyushu University: Kyushu Daigaku Sonoda@doc.kyushu-u.ac.jp A specialist on structure
	Hiroshi Higashiyama, Professor Kindai University: Kinki Daigaku h-hirosi@civileng.kindai.ac.jp

Powered by Editorial Manager® and ProduXion Manager® from Aries Systems Corporation

Revised manuscript with changes marked

Click here to view linked References

Effect of Graphene Oxide Nanoparticles on Blast Load Resistance of Steel Fiber Reinforced Concrete

Sittisak Jamnam[a], Buchit Maho[b*], Apisit Techaphatthanakon[a], Chesta Ruttanapun[c], Peerasak Aemlaor[d], Hexin Zhang[e], Piti Sukontasukkul[a],

[a] *Construction and Building Materials Research Center, Department of Civil Engineering, King Mongkut's University of Technology North Bangkok, Bangkok, Thailand*
[b] *Department of Civil Engineering, Faculty of Engineering, Rajamangala University of Technology Phra Nakhon, Bangkok, Thailand*
[c] *Smart Materials Research and Innovation Unit (SMRIU), Faculty of Science, King Mongkut's Institute of Technology Ladkrabang, Chalongkrung Road, Ladkrabang, Bangkok, Thailand*
[d] *Education Division, Chulachomklao Royal Military Academy, Thailand*
[e] *School of Engineering and the Built Environment, Edinburgh Napier University, Edinburgh, Scotland, United Kingdom*

Corresponding author: buchit.m@rmutp.ac.th

Abstract

Concrete structures may occasionally be subjected to both intentional or unintentional explosions which could cause casualties and damage to properties. Advance research on protective structures are important to enhance blast resistance of materials, and to protect life and properties. This study investigated the effect of graphene oxide nanoparticles (GO) on enhancing the blast resistance of fiber reinforced cement mortar (FRM). GO in solution was incorporated in steel fiber reinforced mortar at the rate of 0, 0.025, 0.050, 0.075, and 0.100 % by weight of cement. A series of experiments were carried out consisting of 2 stages: Stage 1) workability, setting time, compressive and flexural strength, and microstructure using SEM and XRD processes, and Stage 2) blasting loading test. The optimum GO dosage giving the highest compressive and flexural strengths from the 1st stage was determined and chosen to continue on the 2nd stage (blast loading test). The blasting tests were performed on panel specimens (500mmx1000mmx60mm) using TNT weighing ½ lb. (226.7 grams) with three different standoff distances of 340, 400, and 460 mm. Results from Stage 1 on both flexural and compression tests indicated an optimum GO content of 0.025% by weight of cement. The workability was found to decrease with the increasing the GO content. The SEM images also revealed that the addition of GO nanoparticles reduced the porosity in the mortar matrix. For the blasting test, three damage patterns were observed: complete flexural failure, partial damage (flexural cracking), and no major damage, depending on the standoff distance and specimen type. The addition of GO can reduce the maximum and permanent deflections of the panel under blast loading. FRM panels with GO at 0.025% tested at the standoff distance of 460 mm showed the lowest level of damage.

Keywords: Graphene oxide, Steel fiber, Fiber reinforced mortar, Blast resistance, Blast loading, TNT, Non-contact detonation.

1. Introduction

Blasting and explosive events can be a result of unintentional accidents or human negligence, or intentional actions such as terrorist attacks. Terrorists use explosions in several forms such as car bombs, hand grenades, or even package deliveries. The immediate blast can cause casualties to people and also create additional hazards from airborne dust, flying debris, and surface contamination. To prevent damage and protect people, blast resistance structures are essential.

Cement materials are the most commonly used construction material worldwide due to their cost effectiveness, availability and excellent mechanical properties. However, there is also a drawback in these properties in terms of the brittleness and poor tensile strength. To improve the brittleness, short fibers can be randomly incorporated into the concrete mix which can improve the mechanical properties and toughness of cement-based materials [1]-[10], as well as improve several other properties such as fire resistance [11], durability [12], or microparticle infiltration ability [13]. In the case of impact loading or blast resistance, fiber reinforced concrete (FRC) has proven to be superior to plain concrete [14]-[23]. Niş et al. [24][25] indicated that the addition of short and long steel fibers at 1% by volume fraction enhanced the impact energy absorption of concrete by 20.5 and 64 times, respectively. This is due to the fiber bridging effect at crack surfaces, fiber reinforcement is effective in improving the energy absorption capacity of concrete under impaction [26].

Recently, the application of micro and nanomaterials as an additive to enhance material properties has grown in popularity. Their applications are widely accepted in several fields such as food production [27], medical and biomedical applications [28][29], and the environment [30][31]. In the case of construction materials, additive materials in form of micro and nanomaterials have also been widely adapted to enhance properties of cement and concrete. For example, carbon nanotubes to enhance mechanical and electrical resistivity properties [32]-[35], pozzolanic materials to improve cement microstructure and related properties [36]-[39], phase change materials to improve thermal properties [40]-[45], graphene oxide to improve bond strength of FRC [46][47], viscoelastic polymer to increase damping and reduce vibration in concrete structures [48], and nano-silica to improve durability [49], bond strength [50], and mechanical performance [51].

Graphene oxide (GO) is a type of nanomaterial made from a compound of carbon, oxygen, and hydrogen in variable ratios, it is obtained by treating graphite with strong oxidizers and acids to resolve extra metals. The microstructure of graphene oxide is commonly found to be a single layer sheet of the carbon atom in 2-dimensions. It exhibits high specific surface area and excellent mechanical, thermal, and electrical conductivity properties [52][53]. Previous studies have indicated that the application of GO in cement mortar can lead to improvements in mechanical and physical properties of cement composite [54]. However, there was a drawback due to its high specific surface area – the strong van der Waals force between the graphene sheets, and also the hydrophobic nature, made it difficult to obtain uniform dispersion of GO in the concrete [54][55]. To fully utilize GO benefits in cement, several dispersion techniques have been attempted. Jing et al. [56] employed a direct mixing process with GO content of 0.4 wt% which led to a decrease in flowability. Li et al. [57] used the technique for dispersion of graphene in water with the ultrasonication process. They found that a small dosage of GO can enhance both compressive and flexural strength of cement mortar. The nanoparticle filling effect of GO caused a decrease in porosity, an increase in density, and an improvement in restraining crack propagation [58]-[60]. Also, the large specific surface area helped improve internal contact and friction in the cement matrix [61][62].

In the case of impact or blast loading, there are a number of studies on the effect of GO on concrete or FRC subjected to impact or high strain rate of loading. For example, Dong et al. [54] investigated impact resistance of concrete mixed with graphene nanoplate and found that the samples with graphene nanoplate exhibited less damage from impact loading than the samples without. Wang et al. [63] and Li et al. [64] used a Split Hopkinson Pressure bar (SHP) to investigate the dynamic response of cement mortar mixed with GO. They found an increase in dynamic factor, and compressive and splitting tensile strengths in the samples with GO.

Based on the above literature review, even though there are a number of studies investigating the ability of GO in enhancing properties of cement material under high rates of loading, none have carried out tests with the actual explosive materials like Trinitrotoluene (TNT). This research aims to investigate the effect of GO on the blast resistance of FRC using TNT detonated under non-contact conditions. Four types of specimens were prepared, plain mortar (M), mortar mixed with graphene (MG), fiber reinforced mortar (FRM), and FRM mixed with GO (FRMG). The blast loading test was carried out under a non-contact TNT detonating condition. The investigation also included assessing basic mechanical properties such as compressive and flexural strength, and also microstructure using SEM and XRD. The results were analyzed and discussed in terms of failure pattern and level of protection due to blast resistance.

2. Experimental procedure

2.1 Materials

Materials used in this study consisted of Portland cement (ASTM C315), fine aggregate from local river sand with a particle size of 1.19-0.30 mm and size distribution as shown in Figure 1, clean tap water, and steel fiber (hooked-end type) with properties given in Table 1.

The GO was manufactured and produced at the Smart Materials Research and Innovation Unit (SMRIU) at King Mongkut's Institute of Technology Ladkrabang (KMITL) [65]. To prepare the GO solution, the oxidizing graphite was dissolved with a strong acid and oxidizing agent by the modified Hummer's method [66]. In the synthesizing process, the $KMnO_4$ and graphite powder were mixed in a beaker and cooled to 0°C for 10 min. Then, the H_2SO_4 was added while the temperature was maintained at below 15°C. Next, the distilled water was slowly added and stirred, and the temperature was slowly increased up to 95°C over a 60-minute time frame. After the chemical reaction completed, the distilled and H_2O_2 solution was added until the solution color changed to yellow-brown. Centrifugation was used to separate the GO nanosheets and sulphate was removed by washing it with HCl solution. In the purifying process, the GO nanosheets were filtered and washed several times with the distilled water until the pH level reached 7. The GO nanosheets obtained after purification were dried in an oven at 65°C for 24 hours. Before mixing with the mortar, the GO nanosheets powder was dispersed in distilled water with ultrasonication and centrifugation for 90 minutes until the GO solution was uniformly suspended in the solution. The properties of the GO solution are shown in Table 2.

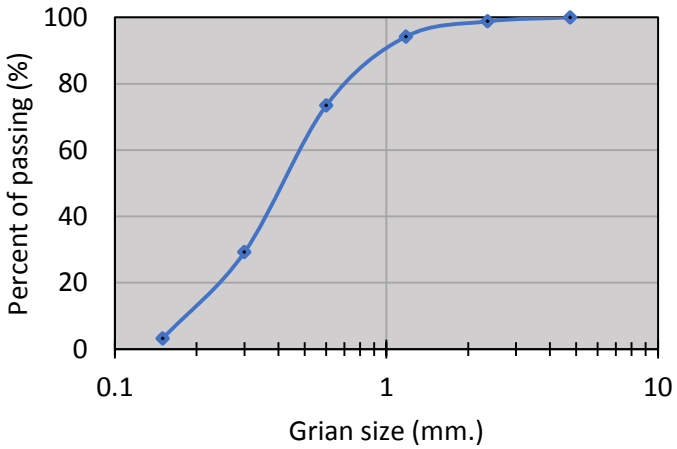

Figure 1. Grain size distribution of sand

Table 1. Properties of steel fiber

Properties	Unit	Description	Appearance
Material	-	Steel	
Type	-	Hooked-end	
Length	mm	35	
Diameter	mm	0.55	
Aspect ratio	-	65	
Elastic modulus	MPa	200,000	
Tensile strength	MPa	1,345	
Strain at ultimate strength	%	0.8	

Table 2. GO solution properties

Name	Graphene oxide solution (GO)
Type	Aqueous suspension
Thickness	Equal to Monolayer sheets of carbon (~0.34nm)
Color	Brown to very dark black
Dispersibility	Polar solvents (DI water)
Concentration	10 mg/mL
specific surface area (BET surface area)	100-200 m^2/ g
Particle size (electron diffraction)	4-6 µm
Characteristics	High mechanical strength and flexibility, dielectric/non-conductivity.

2.2 Mix proportions and specimen preparation

Mix proportions of plain and FRM are shown in Table 3. The water/cement ratio and cement/sand ratio are set at 0.40 and 1:2.75, respectively. Previous research [17], [20][23] [67] indicated that the addition of 2% of steel fibers by volume effectively improved the mechanical properties of cement materials under impact penetration loading. Thus, the mix proportion of FRC in this study was set at 2% by volume. For the ratio of GO solution, evidence from literature recommended GO content not exceeding 0.1% by weight of cement [66][68]. Thus, the amount of GO was set at 0%, 0.025%, 0.050%, 0.075% and 0.100% by weight of cement.

The specimen preparation process began with dry mixing cement and sand for 2 minutes. The liquid part (clean water and GO solution) was mixed together prior to adding to the dry mix. For uniformly dispersed GO, the mixing time was continued for about 3 minutes for all specimen types until the GO was fully dispersed in the fresh mortar. In cases of FRM, the steel fiber was added to the fresh mortar by dividing the fibers into 3 parts. Each part of fiber was distributed to the mixer and mixed continuously for 1 min. The fresh mortar was then cast into steel molds by dividing into 3 layers, compacted on a vibration table for 1 minute, and wrapped in plastic sheeting overnight. After 24 hours, the specimens were demolded and cured under water for 28 days.

Table 3. Mix proportion

Designation	Description	GO (% by weight of cement)	Steel fiber (% by volume)	Cement	Water	Sand
				(kg/m^3)		
M	Plain mortar	0	0	580	230	1600
25MG	Plain mortar + GO	0.025				
50MG		0.050				
75MG		0.075				

100MG		0.100				
FRM	Fiber reinforced mortar	0	2			
25FRMG	Fiber reinforced mortar + GO	0.025				
50FRMG		0.050				
75FRMG		0.075				
100FRMG		0.100				

2.3 Experimental series

The experiment series is divided into 2 parts: 1) Physical and mechanical properties (setting time, flow test, compressive strength, and flexural strength), and 2) Blast loading test on the selected mix proportions. In addition, the change in microstructure due to the addition of GO was also investigated by using scanning electron microscopy (SEM) and X-ray diffraction (XRD).

2.3.1 Setting time and flow test

Both setting time and flow are important parameters used in determining the workability of graphene mortar. The setting time was carried out in accordance with the ASTM C807 standard using Vicat apparatus [69]. To begin a test, fresh mortar was poured in a testing mold, a Vicat needle was placed on the top surface and then released. The depth of penetration was observed and recorded together with the corresponding time. Both initial and final setting times for each mortar type were recorded.

For the flow test, the test was performed following the ASTM C230 standard using a flow table [70]. The fresh mortar was put into a reverse cone mold and compacted in 2 layers with a tamping rod 20 times/layer. The mold was then lifted slowly and vertically to allow the mortar to flow freely. The flow table was then raised and dropped in the vertical direction 25 times in 15 seconds. Finally, the flow diameter was measured in four perpendicular directions and used in calculating the average value.

2.3.2 Compressive and Flexural strength

A compressive strength test was carried out according to ASTM C39 [71] using cylindrical shaped specimens with a diameter of 100 mm and height of 200 mm. The rate of loading was controlled at 0.25±0.05 MPa/s. For the flexural strength, the specimens were cast in a prism shape with dimensions of 100 x 100 x 350 mm, in accordance with ASTM C1609 [72]. The rate of loading for the flexural test was set at 0.05 mm/min with a third-point loading pattern.

2.3.3 Blast loading test

Using the results from 2.3.2, the mix proportion with the highest compressive and flexural strengths was selected for the blasting test. The specimens were prepared in a panel form with dimensions of 500 mm x 1000 mm and thickness of 60 mm. The panel was reinforced with 6 mm-diameter round steel bars with 200 mm spacing as shown in Figure 2. To setup a test, a panel was placed and secured on the steel support (Figure 3), an explosive material (Trinitrotoluene, TNT) weighing 230 g (0.50 lb) was placed on temporary plastic supports with three different vertical standoff distances of 340, 400, and 460 mm (equivalent to blast incident pressure of 4090, 3094, and 2392 kPa, respectively). The antenna, used for measuring the deflection of the panel during the blast event, was securely installed at the bottom of the slab. Before igniting the TNT, the surrounding area was cleared and all personnel were relocated behind the bunker. An electrical detonator (electric blasting cap) was connected to the TNT and ignited using a 12V battery. After the explosion, the damage to the panel, permanent deflection, and maximum deflection were recorded and analyzed [73].

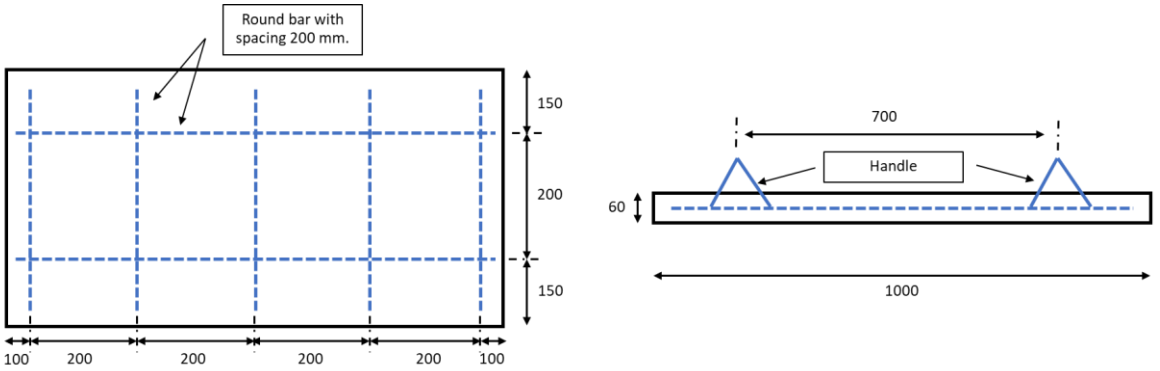

Figure 2. Steel reinforcement of specimen (unit in mm)

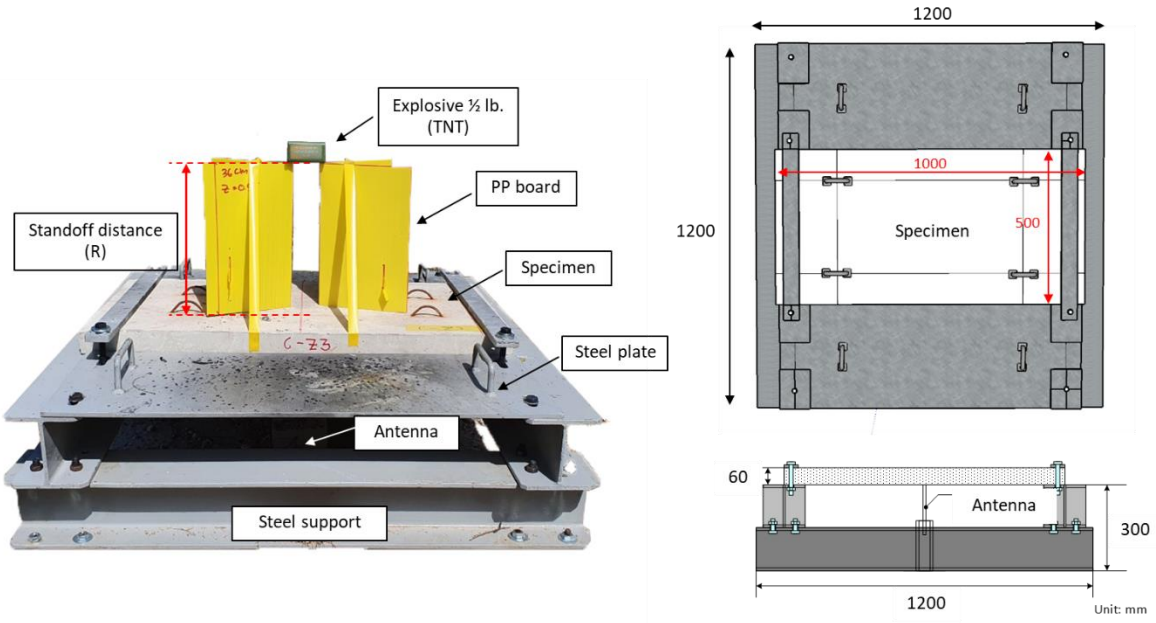

Figure 3. Blast impaction test setup (unit in mm)

4. Results and discussions

4.1 Physical and mechanical properties

4.1.1 Flowability and time of setting

The flow diameter was found to decrease with increasing GO content in both MG and FRMG, as shown in Figure 4. Comparing between FRMG and MG at the same GO content, the FRMG exhibited smaller flow diameter than MG because the existence of fibers interfered with workability of fresh mortar led to the decrease in flow diameter. For effect of GO on plain mortar and FRM, the flow diameter decreased by about 9% and 16% compared with non-GO mortar and FRM respectively. Similar findings were also reported [74]-[76], in that the addition of GO in the mortar lead to a decrease in workability of up to 27% due to the high specific surface area. This is because the addition of GO increases the water requirement of the mix which led to the decrease in free water available to mobilize the fresh mortar. In addition, the hydrophilic functional group and agglomeration of GO trapped the free water in the fresh cement matrix and reduced workability [77]-[80].

For the setting time, the addition of GO led to a slight decrease in initial and final setting times for both MG and FRMG (Figure 5). Wang [81] found that the addition of GO can accelerate the early stage of the hydration reaction due to the filling and nucleation effect of nanoparticles. The addition of high specific surface area materials like GO also caused difficulty in achieving a uniform dispersion in the cement matrix [62]. Comparing between MG and FRMG, the setting time of FRMG was found to almost identical to that of MG (Figure 5a).

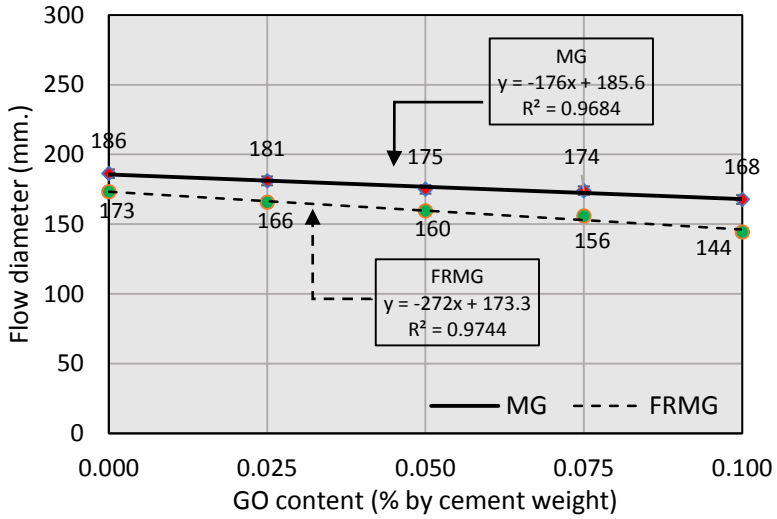

Figure 4. Flow diameter

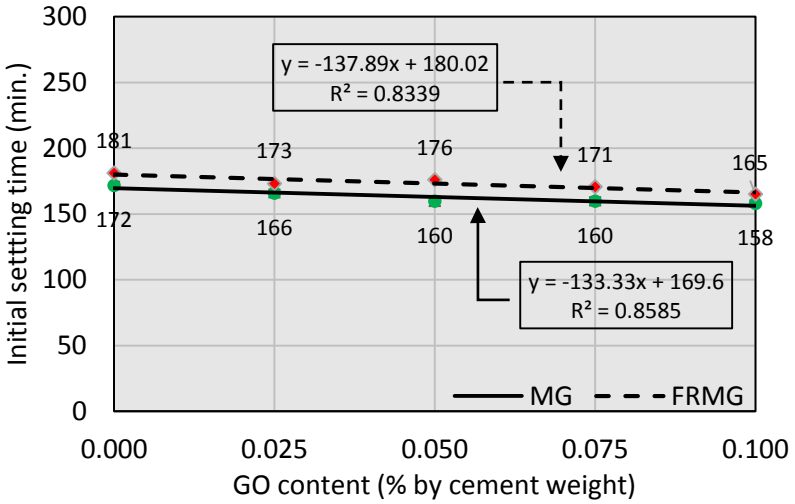

(a) Initial setting time

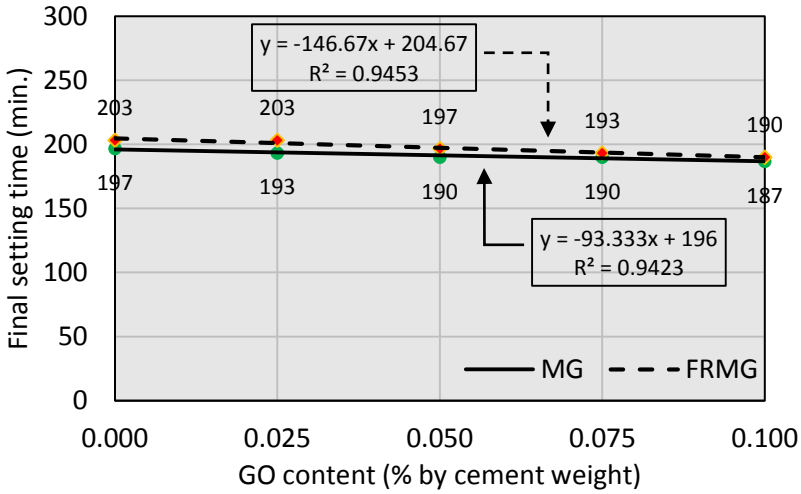

(b) Final setting time

Figure 5. Setting time

4.1.2 Compressive and flexural strength

The failure pattern of MG and FRMG under the compressive and flexural tests are shown in Figures 6 and 7. Under both compression and flexural loads, the plain mortar (M) specimens were found to fail in a brittle failure mode with large cracks running and propagating through the specimen's thickness. Although GO has excellent flexibility, the addition of GO provides no improvement in the ductility of MG as it failed under brittle mode similar to that of plain mortar (M). For FRM and FRMG, the ductile failure patterns were characterized by large numbers of small- and micro-cracks at the outer surface. This was due to the effect of the steel fibers bridging over the cracks, slowing down crack propagation, and preventing the specimen's disintegration.

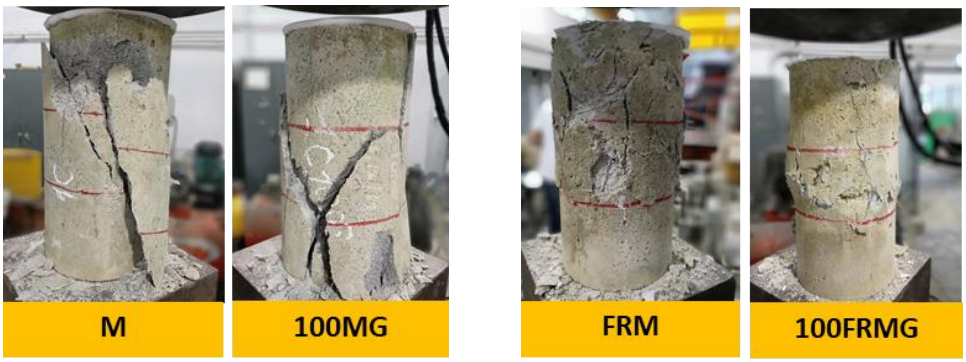

(a) (b)

Figure 6. Compression failure patterns: (a) brittle and (b) ductile modes

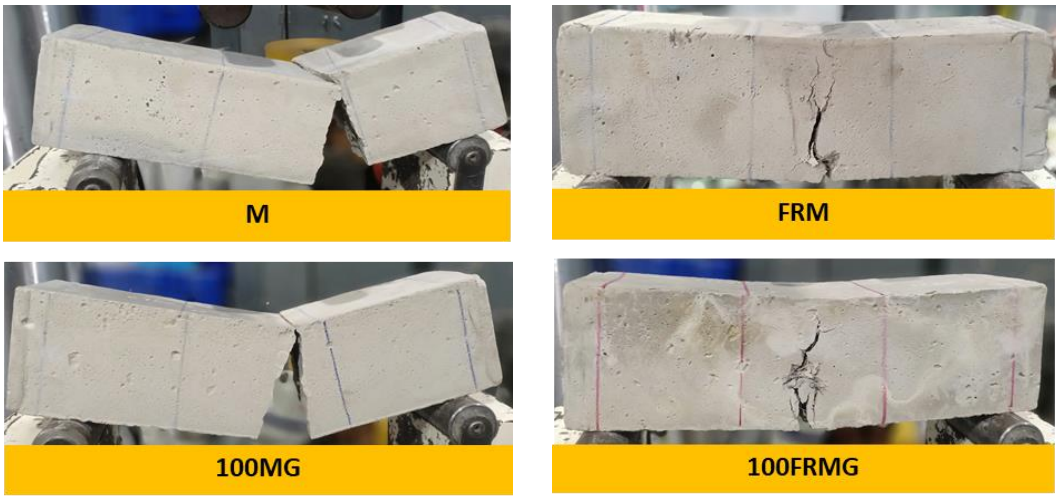

(a) (b)

Figure 7. Flexural failure patterns: (a) brittle and (b) ductile

The effects of GO on compressive and flexural strength are shown in Figures 8 and 9. For both loading types, the optimum GO content was observed to be 0.025%. The highest increase in compressive and flexural strength of 8% and 7% was observed in 25MG. This contributed to the filling effect and the improvement in bonding between the GO and mortar matrix [81][82].

On the other hand, the increase in GO dosage over the optimum content (0.025%) led to a decrease in strength. This was due to an increase in specific surface area from adding GO nanoparticles which caused difficulties in mixing and obtaining good compaction. Similarly, Qureshi et al. [83] found that 0.02% of graphene by cement weight was optimal to give the maximum compressive and flexural strengths, and if the addition of graphene exceeded 0.02%, the strength also decreased gradually.

In the case of FRMG, regardless of the GO content, the compressive strength of FRMG was slightly lower than MG in all cases. This was because large numbers of fibers (at high content of 2%)

lowered the workability which caused poor compaction and high porosity [84]. The optimum GO content for the FRMG was found to be similar to that of MG which was at 0.025%.

In the case of flexural strength, the results were the opposite of the compressive strength. The flexural strength of FRM and FRMG was higher than that of M and MG regardless of the GO content. This was due to the effect of fiber alignment which were mostly parallel to the stress plane when subjected to flexural loading. Niş et al. [85] reported similarly that the fibers were more aligned and oriented along the casting direction in the specimens with thinner sections than the specimens with deep sections.

Comparing between FRMG, the addition of GO at 0.025% also yielded the highest increase in the flexural strength by about 8.22 %. This was due to better bonding between the fiber and cement matrix as recently reported by Chindaprasirt et al. [46].

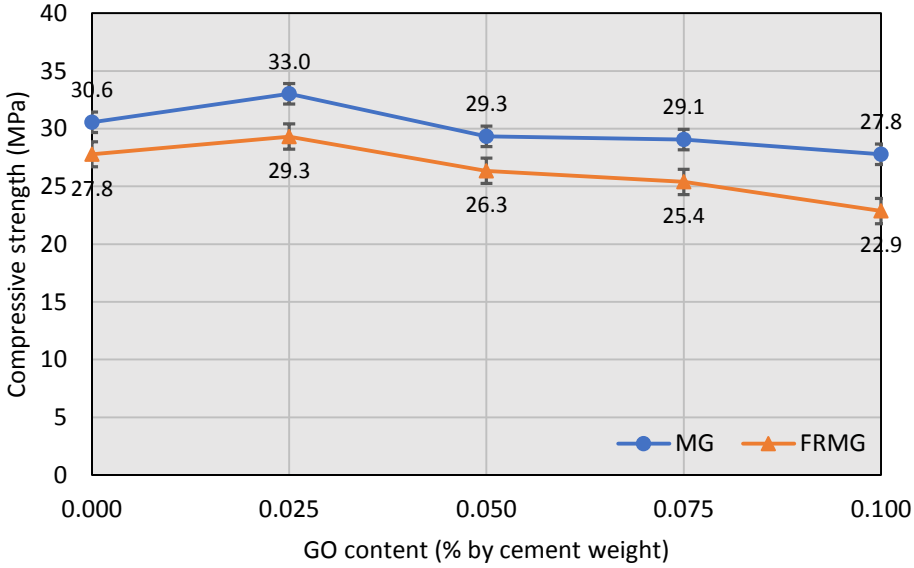

Figure 8. Compressive strength

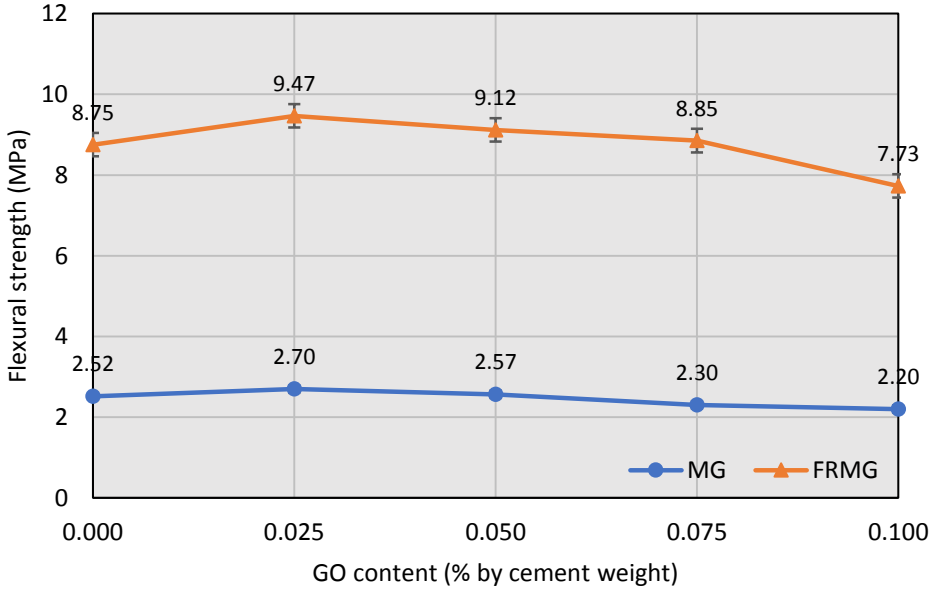

Figure 9. Flexural strength

4.1.3 Microstructure

To study the microstructure and element composition of the mortar with added GO, Scanning Electron Microscope (SEM) and X-ray Diffractometer (XRD) analyses were carried out. The SEM results in Figure 10 show that the addition of GO nanoparticles reduced the porosity of the mortar matrix due to the nano-filter effect [86][88]. Wang et al. [89] showed that the addition of graphene in cement composite can enhance the mechanical properties because nanofibers created crack bridge resistance.

As mentioned earlier, the addition of GO at proportions higher than 0.025% of cement weight led to strength decreases due to the difficulty in mixing and compaction. This can be supported by the results from the SEM images in Figure 10 which showed an increasing number of large voids in the mortar matrix when increasing the GO content higher than 0.025%.

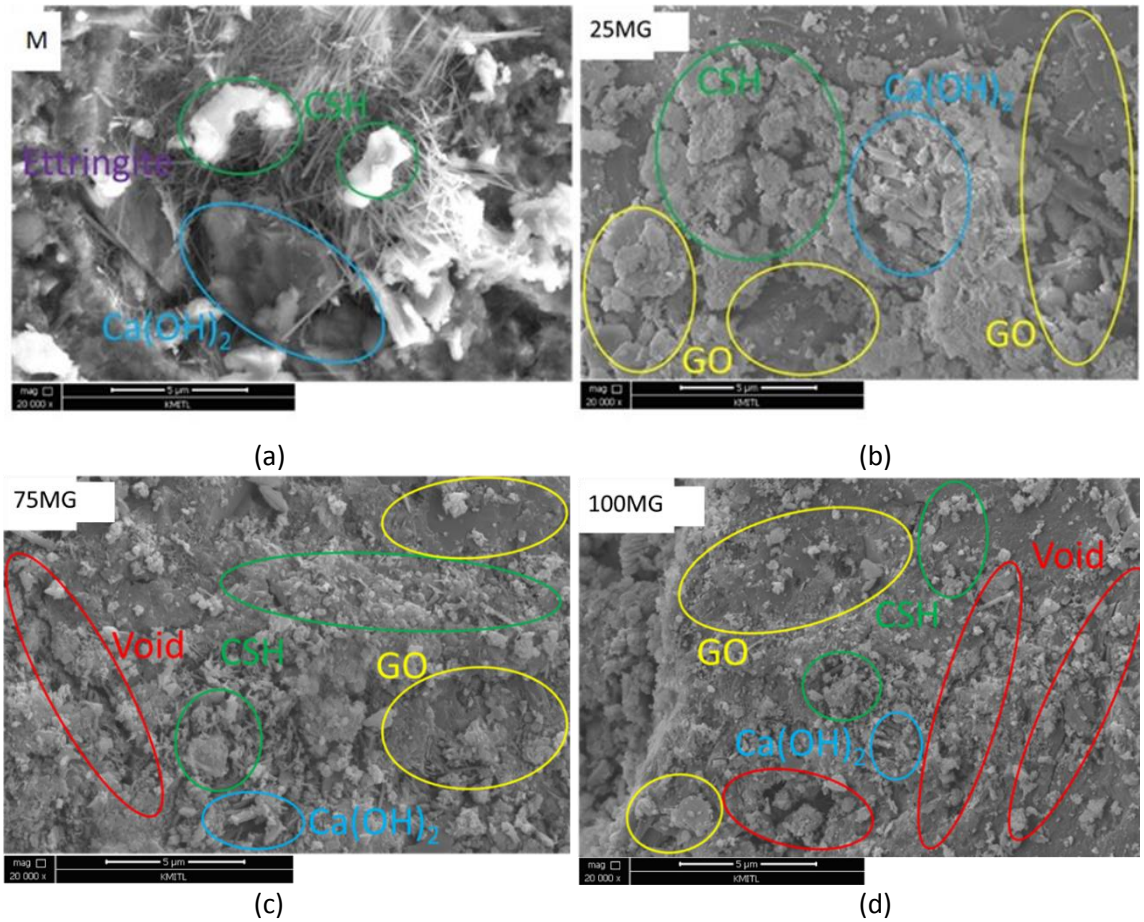

Figure 10. The SEM of mortar mixed with graphene oxide (a) M, (b) 25MG, (c) 75MG, (d) 100MG

The XRD results of mortar incorporated with GO at different dosages are shown in Figure 11. Generally, the hydration products of cement with portlandite (CH), ettringite, dicalcium silicate (C_2S) and tricalcium silicate (C_3S) were detected in mortar with GO dosages. As the XRD results show, the intensity of the peak for the CH phase at position 34.2°, 47.1° and 50.1° increased with increasing GO content indicating the ability of GO to improve cement hydration reaction [66] [83], [90]-[92]. With the increase of hydration reaction, the C_2S and C_3S phases at position 29.5° increased due to the precipitation of CH crystallites [93]. The major peak of quartz at 2-Theta of 26.7° was found in every GO dosage, relating to the mix proportion of sand [88].

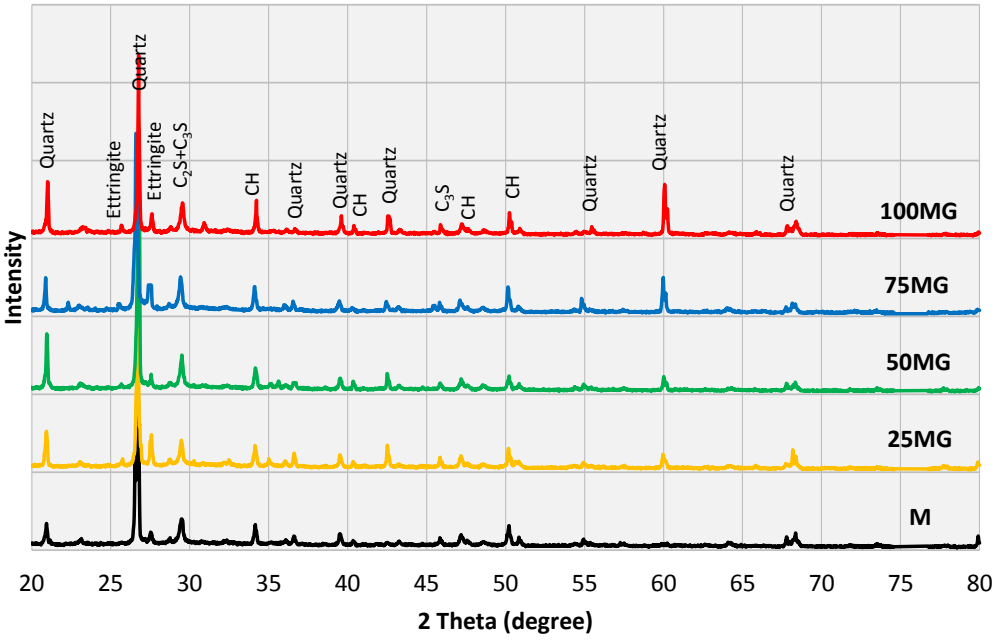

Figure 11. XRD pattern of MG

4.2 Blast loading test

Using the results obtained from 4.1.2, the optimum GO content of 0.025% by weight of cement was concluded for both MG and FRMG. Therefore, it was selected for the blast loading test. The test was performed on plain mortar (M), FRM and 25FRMG to investigate the effect of GO on enhancing blast resistance. The results were discussed in terms of failure mode and maximum deflection that occurred during the blast event.

4.2.1 Damage patterns

The damage patterns observed in the blast loading test were found to be strongly affected by the blasting incident pressure (i.e., standoff distance of the TNT) and the specimen types. The damage pattern can be divided into 3 patterns: complete flexural failure, flexural cracking, and no major damage with microcracking, as shown in Figures 12-14 and summarized in Table 4.

For the complete flexural failure mode, a large crack running through the panel's thickness was visibly observed on both the top and bottom surfaces. The failure is caused by a single crack propagating from the bottom surface across the thickness to the top. The burn marks that appeared on the top surface were a direct result of TNT exposure. The bottom surface suffered a large flexural crack. This failure pattern was found in plain mortar (M) panels subjected to TNT at every standoff distance (340, 400, and 460 mm) due to the brittleness and poor explosion resistance of the M specimens. In the case of FRM panels, this failure mode was found when the TNT was placed at the standoff distance of 340 mm which was the nearest distance and produced the strongest incident pressure. Even though the fibers were able to enhance blast resistance, they cannot prevent a complete flexural failure from occurring at the standoff distance of 340 mm (incident pressure of 4093 kPa).

The second failure mode was flexural cracking. In this mode, a visible crack was observed at the bottom surface of the panel around and outside the blasting region, and there was no sign of cracks at the top surface. This failure pattern was observed in both the FRM and FRMG which indicated the ability of the fibers to enhance explosive resistance and prevent complete failure from occurring. This mode was observed in FRM and 25FRMG at the standoff distance of 400 mm. At the standoff distance of 340 mm, while the FRM specimen suffered a complete flexural failure mode, the 25FRMG only showed flexural cracking mode. For 25FRMG to show a less severe failure mode at the highest incident

pressure of 4093 kPa (or standoff distance of 340 mm) demonstrates the ability of GO to supplement the blast resistance of FRM and prevent a complete flexural failure mode from occurring. Mindess [94] and Lai [95] indicated that the addition of steel fibers improved the blast resistance of mortar because of the fibers' ability to restrain cracks, prevent catastrophic failure, and minimize flying fragments from the impact load and bending fracture [8][96][99].

With the standoff distance increased to 460 mm, no major damage with microcracking failure mode was observed in both FRM and 25FRMG. Burn marks resulting from direct exposure to the blast loading were observed on the top surface. At the bottom surface, small microcracks were visually observed. Since there is no evidence of cracks at the side view photo (Figure 14), this indicated that these cracks only occurred at the surface but did not propagate through the thickness.

In addition, the ability of the fibers to enhance explosive resistance was partly due to the lesser explosive pressure and the longest standoff distance of 460 mm.

It must be noted here that, in this study, there was no spalling of mortar fragments found in any specimens. This was due to the nature of non-contact explosions. Unlike the contact explosion configuration where the failure mode is often accompanied by perforation, spalling, and flying debris [100]-[104], the non-contact explosion type is less severe.

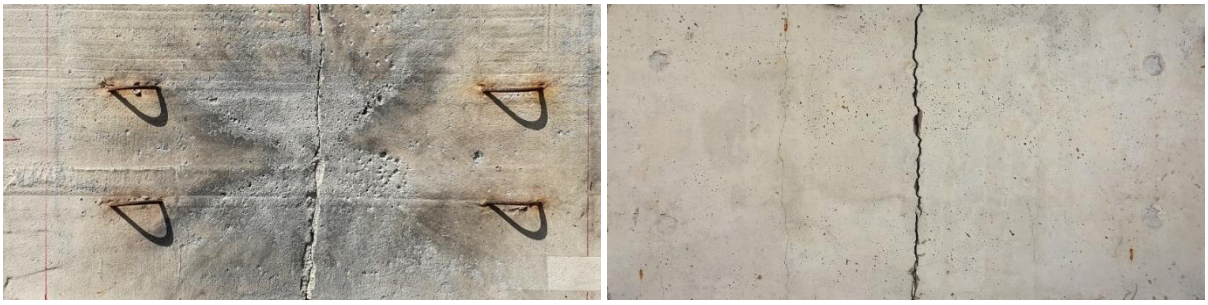

a) Top b) Bottom

c) Side

Figure 12. Complete flexural failure pattern

a) Top b) Bottom

c) Side

Figure 13. Flexural cracking pattern

a) Top b) Bottom

c) Side

Figure 14. No major damage with microcracking pattern

Table 4. Damage patterns

Blast cases	Type	Standoff distance (mm)	Damage pattern
M-R340	Plain mortar (M)	340	Complete flexural failure
M-R400		400	Complete flexural failure
M-R460		460	Complete flexural failure
FRM-R340	Fiber reinforced mortar (FRM)	340	Complete flexural failure
FRM-R400		400	Flexural cracking
FRM-R460		460	No major damage with microcracking
25FRMG-R340	Fiber reinforced mortar with 0.025%wt GO (25FRMG)	340	Flexural cracking
25FRMG-R400		400	Flexural cracking
25FRMG-R460		460	No major damage with microcracking

4.2.2 Maximum and permanent deflections

Results on the maximum and permanent deflections are shown in Figure 15. In general, the typical response of a panel subjected to blast loading includes a downward bending of the panel (to the maximum deflection) during the blasting event and a partial rebound of the panel at the end of the event which leaves behind a permanent deflection. On the effect of standoff distance, both maximum and permanent deflections were found to decrease with the increasing standoff distance. This is clearly because of the decrease in blast incident pressure (from 4090 to 2392 kPa) with the increasing standoff distance of the TNT away from the target (from 340 to 460 mm).

Comparing between M, FRM, and 25FRMG at the same blast incident pressure, both maximum and permanent deflections was highest in M, followed by FRM and finally 25FRMG. This showed that steel fibers were able to increase the blast loading resistance and specimen stiffness and reduce deflections. As for the effect of GO, comparing between FRM and 25FRMG, the maximum deflection was found to be in a similar range when subjected to the same incident pressure. However, in the case

of permanent deflection, 25FRMG exhibited lower permanent deflection than FRM. This is perhaps due to the flexibility of GO and the enhanced bond strength between steel fibers and GO material which allowed the panels to rebound back more effectively and limited the deflection of the specimen, resulting in less permanent deflection[46].

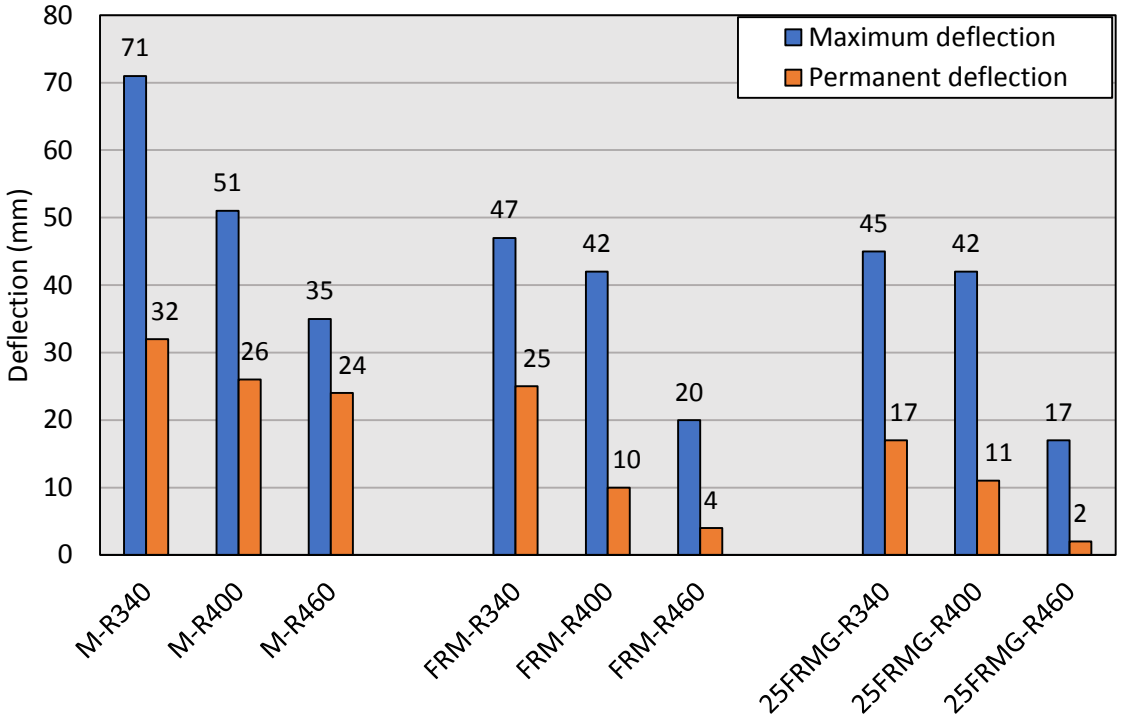

Figure 15. Deflection

5. Conclusions

In this study, the properties and blast resistance of steel fiber reinforced mortar incorporated with GO at 0-0.1% were investigated. The optimum dosage of graphene oxide was determined and blast loading test was carried out using TNT detonated under non-contact condition. Based on the obtained experimental results, the conclusion can be summarized as follows:

- The workability and setting time of mortar decreases with increasing graphene oxide dosages due to the increase in specific surface area and the increase in hydration reaction rate from the addition of GO nanoparticles.
- The optimum GO content of 0.025% by cement weight was observed in this study for both MG and FRMG. With GO dosages over 0.025%, the strength was found to decrease gradually.
- The results from both SEM images and XRD supported the findings that the increase in strength was due to the increase in crystallization of portlandite in the cement hydration reaction from the addition of GO.
- The results of the blast loading test demonstrated 3 damage patterns: complete flexural failure, flexural cracking and no major damage with microcracking. The level of damage depended strongly on the standoff distance and specimen type. At the closest standoff distance (highest explosive pressure), both M and FRM failed under complete flexural failure mode, while FRMG suffered less severe damage (flexural cracking). This indicated that GO was able to enhance the blast loading of FRM.
- As for the deflection, the FRMG was found to exhibit less maximum and permanent deflection than both M and FRM. The smaller permanent deflection showed the flexibility of GO and enhanced bond strength between fiber and mortar matrix which allowed the FRMG to rebound more effectively, resulting in less permanent deflection.

6. Acknowledgements

The authors would like to dedicate this work to Lt. Col. Amornthep Somrat for his strong devotion to this research, he will always be in our memories.

The research was funded by the Armament Research Fellowship Program for Enhancement of Armed Forces and National Defense Thailand. The authors would like to acknowledge support from Smart Materials Research and Innovation Unit, KMITL for providing the graphene oxide, Chulachomklao Royal Military Academy for supporting detonation, and also from King Mongkut's University of Technology North Bangkok and Rajamangala University of Technology Phra Nakhon for laboratory support. The last author would like to acknowledge funding from the National Science, Research and Innovation Fund (NSRF) and King Mongkut's University of Technology North Bangkok (KMUTNB) under the contract no. KMUTNB-FF-66-02. Special thank is also to Ruth Saint for proofreading the manuscript.

7. References

[1] P. Sukontasukkul, "Tensile behaviour of hybrid fibre-reinforced concrete," Advances in Cement Research, vol. 16, no. 3, pp. 115-122, 2004. https://doi.org/10.1680/adcr.2004.16.3.115

[2] P. Jamsawang, T. Suansomjeen, P. Sukontasukkul, P. Jongpradist and D. T.Bergado, "Comparative flexural performance of compacted cement-fiber-sand," Geotextiles and Geomembranes, vol. 46, no. 4, pp. 414-425, 2018. https://doi.org/10.1016/j.geotexmem.2018.03.008

[3] C. Chaikaew, P. Sukontasukkul, U. Chaisakulkiet, V. Sata and P. Chindaprasirt, "Properties of Concrete Pedestrian Blocks Containing Crumb Rubber from Recycle Waste Tyres Reinforced with Steel Fibres," Case Studies in Construction Materials, vol. 11, e00304, 2019. https://doi.org/10.1016/j.cscm.2019.e00304

[4] P. Sukontasukkul, P. Chindaprasirt, P. Pongsopha, T. Phoo-ngernkham, W. Tangchirapat and N. Banthia, "Effect of fly ash/silica fume ratio and curing condition on mechanical properties of fiber-reinforced geopolymer," Journal of Sustainable Cement-Based Materials, vol. 9, no. 4, pp. 1-15, 2020. https://doi.org/10.1080/21650373.2019.1709999

[5] P. Nuaklong, A. Wongsa, K. Boonserm, C. Ngohpok, P. Jongvivatsakul, V. Sata, P. Sukontasukku and P. Chindaprasirt, "Enhancement of mechanical properties of fly ash geopolymer containing fine recycled concrete aggregate with micro carbon fibe," Journal of Building Engineering, vol. 41, 102403, 2021. https://doi.org/10.1016/j.jobe.2021.102403

[6] D.-Y. Yoo, J. Je, H.-J. Choi and P. Sukontasukkul, "Influence of embedment length on the pullout behavior of steel fibers from ultra-high-performance concrete," Materials Letters, vol. 276, 128233, 2020. https://doi.org/10.1016/j.matlet.2020.128233

[7] P. Sukontasukkul, U. Chaisakulkiet, P. Jamsawang, S. Horpibulsuk, C. Jaturapitakkul and P. Chindaprasirt, "Case investigation on application of steel fibers in roller compacted concrete pavement in Thailand," Case Studies in Construction Materials, vol. 11, e00271, 2019. https://doi.org/10.1016/j.cscm.2019.e00271

[8] M. Sappakittipakorn, P. Sukontasukkul, H. Higashiyama and PrinyaChindaprasirt, "Properties of Hooked End Steel Fiber Reinforced Acrylic Modified Concrete," Construction and Building Materials, vol. 186, pp. 1247-1255, 2018. https://doi.org/10.1016/j.conbuildmat.2018.08.055

[9] R. Wongruk, S. Songpiriyakij, P. Sukontasukkul and P. Chindaprasirt, "Properties of Steel Fiber Reinforced Geopolymer," Key Engineering Materials, vol. 659, pp. 143-148, 2015. https://doi.org/10.4028/www.scientific.net/KEM.659.143

[10] M. Jamnongwong, K. Krairan, H. Poorahong, P. Sukontasukkul and P. Jamsawang, "Effect of fiber types on flexural performance of compacted cement-fiber-sand," Suranaree Journal of Science & Technology , vol. 26, no. 4, pp. 421-428, 2019.

[11] P. Sukontasukkul, S. Jamnam, M. Sappakittipakorn, K. Fujikake and P. Chindaprasirt, "Residual flexural behavior of fiber reinforced concrete after heating," Materials and Structures, vol. 51, p. 98, 2018. https://doi.org/10.1617/s11527-018-1210-3

[12] W. Wongprachum, M. Sappakittipakorn, P. Sukontasukkul, P. Chindaprasirt and N. Banthia, "Resistance to sulfate attack and underwater abrasion of fiber reinforced cement mortar," Construction and Building Materials, vol. 189, pp. 686-694, 2018. https://doi.org/10.1016/j.conbuildmat.2018.09.043

[13] T. N. H. Tran, A. Puttiwongrak, P. Pongsopha, D. Intarabut, P. Jamsawang and P. Sukontasukkul, "Microparticle filtration ability of pervious concrete mixed with recycled synthetic fibers," Construction and Building Materials, vol. 270, p. 121807, 2021. https://doi.org/10.1016/j.conbuildmat.2020.121807

[14] D.-Y. Yoo and N. Banthia, "Mechanical properties of ultra-high-performance fiber-reinforced concrete: A review," Cement and Concrete Composites, vol. 73, pp. 267-280, 2016. https://doi.org/10.1016/j.cemconcomp.2016.08.001

[15] D.-Y. Yoo and N. Banthia, "Impact resistance of fiber-reinforced concrete – A review," Cement and Concrete Composites, vol. 104, p. 103389, 2019. https://doi.org/10.1016/j.cemconcomp.2019.103389.

[16] P. Sukontasukkul, S. Mindess, N. Banthia and T. Mikami, "Impact resistance of laterally confined fibre reinforced concrete plates," Materials and Structures, vol. 34, no. 10, pp. 612-618, 2001. https://doi.org/10.1007/BF02482128

[17] P. Sukontasukkul, S. Jamnam, K. Rodsin and N. Banthia, "Use of rubberized concrete as a cushion layer in bulletproof fiber reinforced concrete panels," Construction and Building Materials, vol. 41, pp. 801-811, 2013. https://doi.org/10.1016/j.conbuildmat.2012.12.068

[18] P. Sukontasukkul and S. Mindess, "The shear fracture of concrete under impact loading using end confined beams," Materials and Structures, vol. 36, no. 6, pp. 372-378, 2003. https://doi.org/10.1007/BF02481062

[19] P. Sukontasukkul, S. Jamnam, M. Sappakittipakorn and N. Banthia, "Preliminary study on bullet resistance of double-layer concrete panel made of rubberized and steel fiber reinforced concrete," Materials and Structures, vol. 47, pp. 1-2, 2012. https://doi.org/10.1617/s11527-013-0049-x

[20] B. Maho, P. Sukontasukkul, S. Jamnam, E. Yamaguchi, K. Fujikake and N. Banthia, "Effect of rubber insertion on impact behavior of multilayer steel fiber reinforced concrete bulletproof panel," Construction and Building Materials, vol. 216, pp. 476-484, 2019. https://doi.org/10.1016/j.conbuildmat.2019.04.243

[21] P. Sukontasukkul, S. Mindess and N. Banthia, "Penetration resistance of hybrid fibre reinforced concrete under low velocity impact loading," in Annual Conference of the Canadian Society for Civil Engineering, Canada, 2002.

[22] B. Maho, S. Jamnam, P. Sukontasukkul, K. Fujikake and N. Banthia, "Preliminary Study on Multilayer Bulletproof Concrete Panel: Impact Energy Absorption and Failure Pattern of Fibre Reinforced Concrete, Para-Rubber and Styrofoam Sheets," Procedia Engineering, vol. 210, pp. 369-376, 2017. https://doi.org/10.1016/j.proeng.2017.11.090.

[23] S. Jamnam, B. Maho, A. Techaphatthanakon, Y. Sonoda, D. Y. Yoo and P. Sukontasukkul, "Steel fiber reinforced concrete panels subjected to impact projectiles with different caliber sizes and muzzle energies," Case Studies in Construction Materials, vol. 13, 2020. https://doi.org/10.1016/j.cscm.2020.e00360

[24] A. Niş, N. A. Eren, and A. Çevik, "Effects of recycled tyre rubber and steel fibre on the impact resistance of slag-based self-compacting alkali-activated concrete," Eur. J. Environ. Civ. Eng., vol. 0, no. 0, pp. 1–19, 2022, https://doi.org /10.1080/19648189.2022.2052967.

[25] A. Niş, N. A. Eren, and A. Çevik, "Effects of nanosilica and steel fibers on the impact resistance of slag based self-compacting alkali-activated concrete," Ceram. Int., vol. 47, no. 17, pp. 23905–23918, 2021, https://doi.org/10.1016/j.ceramint.2021.05.099.

[26] D.-Y. Yoo, N. Banthia and Y.-S. Yoon, "Impact Resistance of Reinforced Ultra-High-Performance Concrete Beams with Different Steel Fibers," ACI Structural Journal, vol. 114, no. 1, pp. 113-124, 2017. http://dx.doi.org/10.14359/51689430

[27] K. Neme, A. Nafady, S. Uddin and Y. B.Tola, "Application of nanotechnology in agriculture, postharvest loss reduction and food processing: food security implication and challenge," Heliyon, vol. 7, no. 12, e08539, 2021. https://doi.org/10.1016/j.heliyon.2021.e08539

[28] S. Bokka and A. Chowdhury, "Evolving Trends of Nanotechnology for Medical and Biomedical Applications: A Review," in Module in Materials Science and Materials Engineering, Elsevier, 2021. https://doi.org/10.1016/B978-0-12-820352-1.00098-5.

[29] V. Leso, L. Fontana and I. Iavicoli, "Biomedical nanotechnology: Occupational views," Nano Today, vol. 24, pp. 10-14, 2019. https://doi.org/10.1016/j.nantod.2018.11.002.

[30] A. P. Tom, "Nanotechnology for sustainable water treatment – A review," Materials Today: Proceedings, 2021. https://doi.org/10.1016/j.matpr.2021.05.629.

[31] S. A. Bha, F. Sher, M. Hameed, O. Bashir, R. Kumar, D.-V. N. Vo, P. Ahmad and E. C. Lima, "Sustainable nanotechnology based wastewater treatment strategies: achievements, challenges and future perspectives," Chemosphere, vol. 288 part 3, 2022. 132606. https://doi.org/10.1016/j.chemosphere.2021.132606.

[32] B. Maho, P. Sukontasukkul, G. Sua-Iam, M. Sappakittipakorn, D. Intarabut, C. Suksiripattanapong, P. Chindaprasirt and S. Limkatanyu, "Mechanical properties and electrical resistivity of multiwall carbon nanotubes incorporated into high calcium fly ash geopolymer," Case Studies in Construction Materials, vol. 15, 2021. e00785. https://doi.org/10.1016/j.cscm.2021.e00785.

[33] P. Nuaklong, N. Boonchoo, P. Jongvivatsakul, T. Charinpanitkul and P. Sukontasukkul, "Hybrid effect of carbon nanotubes and polypropylene fibers on mechanical properties and fire resistance of cement mortar," Construction and Building Materials, vol. 275, 122189, 2021.

[34] K. Loamrat, M. Sappakittipakorn and P. Sukontasukkul, "Electrical Resistivity of Cement-Based Sensors under a Sustained Load," Advanced Materials Research, Vols. 931-932, pp. 436-440, 2014.

[35] K. Loamrat, M. Sappakittipakorn and P. Sukontasukkul, "Application of Cement-Based Sensor on Compressive Strain Monitoring in Concrete Members," Advanced Materials Research, Vols. 931-932, pp. 446-450, 2014. https://doi.org/10.4028/www.scientific.net/AMR.931-932.446

[36] S. Dueramaea, W. Tangchirapat, P. Chindaprasirt, C. Jaturapitakkul and P. Sukontasukkul, "Autogenous and drying shrinkages of mortars and pore structure of pastes made with activated binder of calcium carbide residue and fly ash," Construction and Building Materials, vol. 230, 116962, 2020. https://doi.org/10.1016/j.conbuildmat.2019.116962

[37] S. Hanjitsuwan, B. Injorhor, T. Phoo-ngernkham, N. Damrongwiriyanupap, L.-Y. Li, P. Sukontasukkul and P. Chindaprasirt, "Drying shrinkage, strength and microstructure of alkali-activated high-calcium fly ash using FGD-gypsum and dolomite as expansive additive," Cement and Concrete Composites, vol. 114, 103760, 2020. https://doi.org/10.1016/j.cemconcomp.2020.103760

[38] S. Dueramae, W. Tangchirapat, P. Sukontasukkul, P. Chindaprasirtd and C. Jaturapitakkul, "Investigation of compressive strength and microstructures of activated cement free binder from fly ash - calcium carbide residue mixture," Journal of Materials Research and Technology, vol. 8, no. 5, pp. 4757-4765, 2019. https://doi.org/10.1016/j.jmrt.2019.08.022

[39] A. Wongsa, A. Siriwattanakarn, P. Nuaklong, V. Sata, P. Sukontasukkul and P. Chindaprasirt, "Use of recycled aggregates in pressed fly ash geopolymer concrete," Environmental Progress & Sustainable Energy, vol. 39, no. 2, e13327, 2019. https://doi.org/10.1002/ep.13327

[40] P. Sukontasukkul, N. Nontiyutsirikul, S. Songpiriyakij, K. Sakai and P. Chindaprasirt, "Use of phase change material to improve thermal properties of lightweight geopolymer panel," Materials and Structures, vol. 49, p. 4637–4645, 2016.

[41] P. Sukontasukkul, T. Sutthiphasilp, C. Wonchalerm and P. Chindaprasirt, "Improving thermal properties of exterior plastering mortars with phase change materials with different melting temperatures: paraffin and polyethylene glycol," Advances in Building Energy Research, vol. 13, no. 1, pp. 1-21, 2018.

[42] P. Sukontasukkul, E. Intawong, P. Preemanoch and P. Chindaprasirt, "Use of paraffin impregnated lightweight aggregates to improve thermal properties of concrete panels," Materials and Structures, vol. 49, pp. 1793-1803, 2016.

[43] P. Uthaichotirat, P. Sukontasukkul, P. Jitsangiam, Cherdsak, Suksiripattanapong, V. Sata and P. Chindaprasirt, "Thermal and sound properties of concrete mixed with high porous aggregates from manufacturing waste impregnated with phase change material," Journal of Building Engineering, vol. 29, 101111, 2020. https://doi.org/10.1016/j.jobe.2019.101111

[44] P. Sukontasukkul, T. Sangpet, M. Newlands, D.-Y. Yoo, W. Tangchirapat, S. Limkatanyu and P. Chindaprasirt, "Thermal storage properties of lightweight concrete incorporating phase change materials with different fusion points in hybrid form for high temperature applications," Heliyon, vol. 6, no. 9, e04863, 2020. https://doi.org/10.1016/j.heliyon.2020.e04863

[45] P. Pongsopha, P. Sukontasukkul, TanakornPhoo-ngernkham, T. Imjai, P. Jamsawang and P. Chindaprasirt, "Use of burnt clay aggregate as phase change material carrier to improve thermal properties of concrete panel," Case Studies in Construction Materials, vol. 11, e00242, 2019. https://doi.org/10.1016/j.cscm.2019.e00242.

[46] P. Chindaprasirt, P. Sukontasukkul, A. Techaphatthanakon, S. Kongtun, C. Ruttanapun, D.-Y. Yoo, W. Tangchirapat, S. Limkatanyu and N. Banthia, "Effect of graphene oxide on single fiber pullout behavior," Construction and Building Materials, vol. 280, 122539, 2021. https://doi.org/10.1016/j.conbuildmat.2021.122539

[47] D. Intarabut, P. Sukontasukkul, T. Phoo-Ngernkham, H. Zhang, D.-Y. Yoo, S. Limkatanyu and P. Chindaprasirt, "Influence of Graphene Oxide Nanoparticles on Bond-Slip Reponses between Fiber and Geopolymer Mortar," Nanomaterials, vol. 12, no. 6, p. 943, 2022. https://doi.org/10.3390/nano12060943.

[48] K. Tontiwattanakul, J. Sanguansin, V. Ratanavaraha, V. Sata, S. tLimkatanyu and P. Sukontasukkul, "Effect of viscoelastic polymer on damping properties of precast concrete panel," Heliyon, vol. 7, no. 5, e06967, 2021. https://doi.org/10.1016/j.heliyon.2021.e06967

[49] A. Çevik, R. Alzeebaree, G. Humur, A. Niş, and M. E. Gülşan, “Effect of nano-silica on the chemical durability and mechanical performance of fly ash based geopolymer concrete,” Ceram. Int., vol. 44, no. 11, pp. 12253–12264, 2018, https://doi.org/10.1016/j.ceramint.2018.04.009.

[50] M. E. Gülşan, R. Alzeebaree, A. A. Rasheed, A. Niş, and A. E. Kurtoğlu, “Development of fly ash/slag based self-compacting geopolymer concrete using nano-silica and steel fiber,” Constr. Build. Mater., vol. 211, pp. 271–283, 2019, https://doi.org/10.1016/j.conbuildmat.2019.03.228.

[51] N. A. Eren, R. Alzeebaree, A. Çevik, A. Niş, A. Mohammedameen, and M. E. Gülşan, “Fresh and hardened state performance of self-compacting slag based alkali activated concrete using nanosilica and steel fiber,” J. Compos. Mater., vol. 55, no. 28, pp. 4125–4139, 2021, https://doi.org /10.1177/00219983211032390.

[52] M. Raji, N. Zari, A. e. k. Qaiss and R. Bouhfid, "Chapter 1 - Chemical Preparation and Functionalization Techniques of Graphene and Graphene Oxide," in In Micro and Nano Technologies, Functionalized Graphene properties and its application, Elsevier, 2019, pp. 1-20. https://doi.org/10.1016/B978-0-12-814548-7.00001-5.

[53] B. SA, U. N, B. FA, I. M and S. S., "A review of functionalized graphene properties and its application," International Journal of Innovation Science and Research, vol. 17, 2015. 303e15
[54] W. Dong, W. Li, Y. Guo, K. Wang and D. Sheng, "Mechanical properties and piezoresistive performances of intrinsic graphene nanoplate/cement-based sensors subjected to impact load," Construction and Building Materials, vol. 327, 126978, 2022. https://doi.org/10.1016/j.conbuildmat.2022.126978.
[55] H. Du and S. D. Pang, "Dispersion and stability of graphene nanoplatelet in water and its influence on cement composites," Construction and Building Materials, vol. 167, pp. 403-413, 2018.
[56] G. Jing, Z. Ye, X. Lu and P. Hou, "Effect of graphene nanoplatelets on hydration behaviour of Portland cement by thermal analysis," Advances in Cement Research, vol. 29, no. 2, pp. 63-70, 2016.
[57] X. Li, Z. Lu, S. Chuah, W. Li, Y. Liu and W. Duan, "Effects of graphene oxide aggregates on hydration degree, sorptivity, and tensile splitting strength of cement paste," Composites Part A: Applied Science and Manufacturing, vol. 100, pp. 1-8, 2017
[58] J. An, M. McInnis, W. Chung and B. Nam, "Feasibility of using graphene oxide nanoflake (GONF) as additive of cement composite," Applied Sciences, vol. 8, p. 419, 2018.
[59] K. Gong, Z. Pan, A. Korayem, L. Qiu, D. Li and F. Collins, "Reinforcing effects of graphene oxide on portland cement paste," Journal of Materials in Civil Engineering, vol. 27, 2015. A4014010.
[60] Z. Pan, L. He, L. Qiu, A. Korayem, L. Gang, J. Zhu and F. Collins, "Mechanical properties and microstructure of a graphene oxide-cement composite," Cement and Concrete Composites, vol. 58, pp. 140-147, 2015.
[61] W. Long, Y. Cu, B. Xiao, Q. Zhang and F. Xing, "Micro-mechanical properties and multi-scaled pore structure of graphene oxide cement paste: Synergistic application of nanoindentation, X-ray computed tomography, and SEM-EDS analysis," Construction and Building Materials, vol. 179, pp. 661-674, 2018.
[62] Y. Lin and H. Du, "Graphene reinforced cement composites: A review.," Construction and Building Materials, vol. 265, 2020. 120312. https://doi.org/10.1016/j.conbuildmat.2020.120312
[63] J. Wang, S. Dong, X. Yu and B. Han, "Mechanical properties of graphene-reinforced reactive powder concrete at different strain rates," Journal of Materials Science, vol. 55, p. 3369–3387, 2020. https://doi.org/10.1007/s10853-019-04246-5
[64] C. Y. Li, S. J. Chen, W. G. Li, X. Y. Li, D. Ruan and W. H. Duan, "Dynamic increased reinforcing effect of graphene oxide on cementitious nanocomposite," Construction and Building Materials, vol. 206, pp. 694-702, 2019. https://doi.org/10.1016/j.conbuildmat.2019.02.001
[65] C. Phrompet, C. Sriwong and C. Ruttanapun, "Mechanical, dielectric, thermal and antibacterial properties of reduced graphene oxide (rGO)-nanosized C3AH6 cement nanocomposites for smart cement-based materials," *Composites Part B: Engineering,* vol. 175, 2019. https://doi.org/10.1016/j.compositesb.2019.107128
[66] L. Zhao, X. Guo, L. Song, Y. Song, G. Dai and J. Liu, "An intensive review on the role of graphene oxide in cement-based materials," *Construction and Building Materials,* vol. 241, 2020. https://doi.org/10.1016/j.conbuildmat.2019.117939
[67] R. Sovják, T. Vavřiník, J. Zatloukal, P. Máca, T. Mičunek and M. Frydrýn, "Resistance of slim UHPFRC targets to projectile impact using in-service bullets," *International Journal of Impact Engineering,* vol. 76, pp. 166-177, 2015. https://doi.org/10.1016/j.ijimpeng.2014.10.002
[68] Y. Lin and H. Du, "Graphene reinforced cement composites: A review.," Construction and Building Materials, vol. 265, 2020. 120312. https://doi.org/10.1016/j.conbuildmat.2020.120312
[69] A. C807-21, Standard Test Method for Time of Setting of Hydraulic Cement Mortar by Modified Vicat Needle, West Conshohocken, PA: ASTM International, 2021. www.astm.org

[70] ASTM C230 /. C230M-21, Standard Specification for Flow Table for Use in Tests of Hydraulic Cement, West Conshohocken, PA: ASTM International, 2021. www.astm.org
[71] ASTM C39/. C39M-21, Standard Test Method for Compressive Strength of Cylindrical Concrete Specimens, West Conshohocken, PA: ASTM International, 2021., www.astm.org
[72] ASTM C1609 /. C1609M-19a, Standard Test Method for Flexural Performance of Fiber-Reinforced Concrete (Using Beam With Third-Point Loading), West Conshohocken, PA: ASTM International, 2019 www.astm.org
[73] PDC-TR 06-08, "Single Degree of Freedom Blast Design Spreadsheet (SBEDS) Methodology," U.S. Army Corps of Engineers Protective Design Center Technical Report, 2008.
[74] L. Lu and D. Ouyang, "Properties of cement mortar and ultra-high strength concrete incorporating graphene oxide nanosheets," *Nanomaterials ,* vol. 7, no. 7, 2017. https://doi.org/10.3390/nano7070187
[75] W. J. Long, J. J. Wei, H. Ma and F. Xing, "Dynamic mechanical properties and microstructure of graphene oxide nanosheets reinforced cement composites," *Nanomaterials,* vol. 7, p. 12, 2017. https://doi.org/10.3390/nano7120407
[76] Q. Wang, J. Wang, C.-x. Lu, B.-w. Liu, K. Zhang and C.-z. Li, "Influence of graphene oxide additions on the microstructure and mechanical strength of cement," *New Carbon Materials,* vol. 30, no. 4, pp. 349-356, 2015. ISSN 1872-5805, https://doi.org/10.1016/S1872-5805(15)60194-9.
[77] Z. Pan, L. He, L. Qiu, A. H. Korayem, G. Li, J. W. Zhu, F. Collins, D. Li, W. H. Duan and M. C. Wang, "Mechanical properties and microstructure of a graphene oxide-cement composite," *Cement and Concrete Composites,* vol. 58, pp. 140-147, 2015. https://doi.org/10.1016/j.cemconcomp.2015.02.001
[78] H. Du and S. D. Pang, "Dispersion and stability of graphene nanoplatelet in water and its influence on cement composites," *Construction and Building Materials,* vol. 167, pp. 403-413, 2018. https://doi.org/10.1016/j.conbuildmat.2018.02.046
[79] K. Gong, Z. Pan, A. H. Korayem, L. Qiu, D. Li, F. Collins, C. M. Wang and W. H. Duan, "Reinforcing Effects of Graphene Oxide on Portland Cement Paste," *Journal of Materials in Civil Engineering,* vol. 27, no. 2, 2015. https://doi.org/10.1061/(asce)mt.1943-5533.0001125
[80] B. Wang, R. Jiang and Z. Wu, "Investigation of the mechanical properties and microstructure of graphene nanoplatelet-cement composite," *Nanomaterials,* vol. 6, no. 11, 2016. https://doi.org/10.3390/nano6110200
[81] B. Wang and B. Pang, "Mechanical property and toughening mechanism of water reducing agents modified graphene nanoplatelets reinforced cement composites," *Construction and Building Materials,* vol. 226, pp. 699-711, 2019. https://doi.org/10.1016/j.conbuildmat.2019.07.229
[82] M. Wang, R. Wang, H. Yao, S. Farhan, S. Zheng and C. Du, "Study on the three dimensional mechanism of graphene oxide nanosheets modified cement," *Construction Building Materials,* vol. 126, pp. 730-739, 2016.
[83] T. Qureshi and D. Panesar, "Nano reinforced cement paste composite with functionalized graphene and pristine graphene nanoplatelets," *Composites Part B: Engineering,* 2020. 108063.
[84] S. Sharma and N. Kothiyal, "Comparative effects of pristine and ball-milled graphene oxide on physico-chemical characteristics of cement mortar nanocomposites," *Construction Building Materials,* vol. 115, pp. 256-268, 2016.
[85] A. Niş, N. Özyurt, and T. Özturan, “Variation of Flexural Performance Parameters Depending on Specimen Size and Fiber Properties,” J. Mater. Civ. Eng., vol. 32, no. 4, p. 04020054, 2020, https://doi.org/10.1061/(asce)mt.1943-5533.0003105.
[86] K. Gong, Z. Pan, A. Korayem, L. Qiu, D. Li and F. Collins, "Reinforcing effects of graphene oxide on portland cement paste," *Journal of Materials in Civil Engineering,* vol. 27, 2015. A4014010.

[87] Z. Pan, L. He, L. Qiu, A. H. Korayem, G. Li, J. W. Zhu, F. Collins, D. Li, W. H. Duan and M. C. Wang, "Mechanical properties and microstructure of a graphene oxide–cement composite," *Cement and Concrete Composites,* vol. 58, pp. 140-147, 2015. https://doi.org/10.1016/j.cemconcomp.2015.02.001.

[88] S. Sharma and N. Kothiyal, " Influence of graphene oxide as dispersed phase in cement mortar matrix in defining the crystal patterns of cement hydrates and its effect on mechanical, microstructural and crystallization properties," *RSC Advance,* vol. 5, pp. 52642-52657, 2015.

[89] B. Wang, R. Jiang and Z. Wu, "Investigation of the mechanical properties and microstructure of graphene nanoplatelet-cement composite," *Nanomaterials,* vol. 6, no. 11, p. 200, 2016.

[90] C. Lin, W. Wei and Y. Hu, "Catalytic behavior of graphene oxide for cement hydration process," *The Journal of Physics and Chemistry of Solids,* vol. 89, pp. 128-33, 2016.

[91] T. Qureshi and D. Panesar, "Impact of graphene oxide and highly reduced graphene oxide on cement based composites," *Construction and Building Materials,* vol. 206, pp. 71-83, 2019.

[92] W. Long, T. Ye, Y. Gu, H. Li and F. Xing, "Inhibited effect of graphene oxide on calcium leaching of cement pastes," *Construction and Building Materials,* vol. 202, pp. 177-188, 2019

[93] R. JADHAV and N. C. DEBNATH, "Computation of X-ray powder diffractograms of cement components and its application to phase analysis and hydration performance of OPC cemen," Bulletin of Materials Science, vol. 34, p. 1137–1150, 2011. https://doi.org/10.1007/s12034-011-0134-0

[94] S. Mindess, J. Young and D. Darwin, Concrete, second ed., New Jersey: Pearson Education Inc., 2003.

[95] J. Lai and W. Sun, "Dynamic behaviour and visco-elastic damage model of ultrahigh performance cementitious composite," *Cement and Concrete Research,* vol. 39, no. 11, pp. 1044-1051, 2009.

[96] N. Tran, T. Tran and D. Kim, "; High rate response of ultra-high-performance fiber-reinforced concretes under direct tension,," *Cement and Concrete Research,* vol. 69, pp. 72-87, 2015.

[97] K. Wille, M. Xu, S. El-Tawil and A. Naaman, "Dynamic impact factors of strain hardening UHP-FRC under direct tensile loading at low strain rates," *Materials and Structures,* vol. 49, no. 4, pp. 1351-1365, 2016.

[98] D.Y. Yoo and N. Banthia, "Impact resistance of ultra-high-performance fiber-reinforced concrete with different steel fibers," in *9th RILEM International Symposium on Fiber Reinforced Concrete (BEFIB 2016)*, Pacific Gateway Hotel, Vancouver, BC, Canada, 2016.

[99] P. Sukontasukkul, P. Pongsopha, P. Chindaprasirt and S. Songpiriyakij, "Flexural performance and toughness of hybrid steel and polypropylene fibre reinforced geopolymer," *Construction and Building Materials,* vol. 161, pp. 37-44, 2018. https://doi.org/10.1016/j.conbuildmat.2017.11.122.

[100] D. Yoo, S. Kang and Y. Yoon, "Effect of fiber length and placement method on flexural behavior, tension-softening curve, and fiber distribution characteristics of UHPFRC," *Construction Building Materails,* vol. 64, pp. 67-81, 2014.

[101] D. Yoo, G. Zi, S. Kang and Y. Yoon, " Biaxial flexural behavior of ultra-highperformance fiber-reinforced concrete with different fiber lengths and placement methods," *Cement and Concrete Composites,* vol. 63, pp. 51-66, 2015

[102] J. Li, C. Wu and H. Hao, "Investigation of ultra-high performance concrete slab and normal strength concrete slab under contact explosion," *Engineering Structures,* vol. 102, pp. 395-408, 2015

[103] J. Li, C. Wu, H. Hao, Z. Wang and Y. Su, "Experimental investigation of ultra-high performance concrete slabs under contact explosions," *The International Journal of Impact Engineering,* vol. 93, pp. 62-75, 2016.

[104] H. Y. Grisaro, D. Benamou and A. Mitelman, "Field tests of fiber reinforced concrete slabs subjected to close-in and contact detonations of high explosives," *International Journal of*

Impact Engineering, vol. 162, 2022. 104136.
https://doi.org/10.1016/j.ijimpeng.2021.104136.

Manuscript (For revision, remove the original version and upload clean version of revised paper)

Click here to view linked References

Effect of Graphene Oxide Nanoparticles on Blast Load Resistance of Steel Fiber Reinforced Concrete

Sittisak Jamnam[a], Buchit Maho[b*], Apisit Techaphatthanakon[a], Chesta Ruttanapun[c], Peerasak Aemlaor[d], Hexin Zhang[e], Piti Sukontasukkul[a],

[a] *Construction and Building Materials Research Center, Department of Civil Engineering, King Mongkut's University of Technology North Bangkok, Bangkok, Thailand*
[b] *Department of Civil Engineering, Faculty of Engineering, Rajamangala University of Technology Phra Nakhon, Bangkok, Thailand*
[c] *Smart Materials Research and Innovation Unit (SMRIU), Faculty of Science, King Mongkut's Institute of Technology Ladkrabang, Chalongkrung Road, Ladkrabang, Bangkok, Thailand*
[d] *Education Division, Chulachomklao Royal Military Academy, Thailand*
[e] *School of Engineering and the Built Environment, Edinburgh Napier University, Edinburgh, Scotland, United Kingdom*

Corresponding author: buchit.m@rmutp.ac.th

Abstract

Concrete structures may occasionally be subjected to both intentional or unintentional explosions which could cause casualties and damage to properties. Advance research on protective structures are important to enhance blast resistance of materials, and to protect life and properties. This study investigated the effect of graphene oxide nanoparticles (GO) on enhancing the blast resistance of fiber reinforced cement mortar (FRM). GO in solution was incorporated in steel fiber reinforced mortar at the rate of 0, 0.025, 0.050, 0.075, and 0.100 % by weight of cement. A series of experiments were carried out consisting of 2 stages: Stage 1) workability, setting time, compressive and flexural strength, and microstructure using SEM and XRD processes, and Stage 2) blasting loading test. The optimum GO dosage giving the highest compressive and flexural strengths from the 1st stage was determined and chosen to continue on the 2nd stage (blast loading test). The blasting tests were performed on panel specimens (500mmx1000mmx60mm) using TNT weighing ½ lb. (226.7 grams) with three different standoff distances of 340, 400, and 460 mm. Results from Stage 1 on both flexural and compression tests indicated an optimum GO content of 0.025% by weight of cement. The workability was found to decrease with the increasing the GO content. The SEM images also revealed that the addition of GO nanoparticles reduced the porosity in the mortar matrix. For the blasting test, three damage patterns were observed: complete flexural failure, partial damage (flexural cracking), and no major damage, depending on the standoff distance and specimen type. The addition of GO can reduce the maximum and permanent deflections of the panel under blast loading. FRM panels with GO at 0.025% tested at the standoff distance of 460 mm showed the lowest level of damage.

Keywords: Graphene oxide, Steel fiber, Fiber reinforced mortar, Blast resistance, Blast loading, TNT, Non-contact detonation.

1. Introduction

Blasting and explosive events can be a result of unintentional accidents or human negligence, or intentional actions such as terrorist attacks. Terrorists use explosions in several forms such as car bombs, hand grenades, or even package deliveries. The immediate blast can cause casualties to people and also create additional hazards from airborne dust, flying debris, and surface contamination. To prevent damage and protect people, blast resistance structures are essential.

Cement materials are the most commonly used construction material worldwide due to their cost effectiveness, availability and excellent mechanical properties. However, there is also a drawback in these properties in terms of the brittleness and poor tensile strength. To improve the brittleness, short fibers can be randomly incorporated into the concrete mix which can improve the mechanical properties and toughness of cement-based materials [1]-[10], as well as improve several other properties such as fire resistance [11], durability [12], or microparticle infiltration ability [13]. In the case of impact loading or blast resistance, fiber reinforced concrete (FRC) has proven to be superior to plain concrete [14]-[23]. Niş et al. [24][25] indicated that the addition of short and long steel fibers at 1% by volume fraction enhanced the impact energy absorption of concrete by 20.5 and 64 times, respectively. This is due to the fiber bridging effect at crack surfaces, fiber reinforcement is effective in improving the energy absorption capacity of concrete under impaction [26].

Recently, the application of micro and nanomaterials as an additive to enhance material properties has grown in popularity. Their applications are widely accepted in several fields such as food production [27], medical and biomedical applications [28][29], and the environment [30][31]. In the case of construction materials, additive materials in form of micro and nanomaterials have also been widely adapted to enhance properties of cement and concrete. For example, carbon nanotubes to enhance mechanical and electrical resistivity properties [32]-[35], pozzolanic materials to improve cement microstructure and related properties [36]-[39], phase change materials to improve thermal properties [40]-[45], graphene oxide to improve bond strength of FRC [46][47], viscoelastic polymer to increase damping and reduce vibration in concrete structures [48], and nano-silica to improve durability [49], bond strength [50], and mechanical performance [51].

Graphene oxide (GO) is a type of nanomaterial made from a compound of carbon, oxygen, and hydrogen in variable ratios, it is obtained by treating graphite with strong oxidizers and acids to resolve extra metals. The microstructure of graphene oxide is commonly found to be a single layer sheet of the carbon atom in 2-dimensions. It exhibits high specific surface area and excellent mechanical, thermal, and electrical conductivity properties [52][53]. Previous studies have indicated that the application of GO in cement mortar can lead to improvements in mechanical and physical properties of cement composite [54]. However, there was a drawback due to its high specific surface area – the strong van der Waals force between the graphene sheets, and also the hydrophobic nature, made it difficult to obtain uniform dispersion of GO in the concrete [54][55]. To fully utilize GO benefits in cement, several dispersion techniques have been attempted. Jing et al. [56] employed a direct mixing process with GO content of 0.4 wt% which led to a decrease in flowability. Li et al. [57] used the technique for dispersion of graphene in water with the ultrasonication process. They found that a small dosage of GO can enhance both compressive and flexural strength of cement mortar. The nanoparticle filling effect of GO caused a decrease in porosity, an increase in density, and an improvement in restraining crack propagation [58]-[60]. Also, the large specific surface area helped improve internal contact and friction in the cement matrix [61][62].

In the case of impact or blast loading, there are a number of studies on the effect of GO on concrete or FRC subjected to impact or high strain rate of loading. For example, Dong et al. [54] investigated impact resistance of concrete mixed with graphene nanoplate and found that the samples with graphene nanoplate exhibited less damage from impact loading than the samples without. Wang et al. [63] and Li et al. [64] used a Split Hopkinson Pressure bar (SHP) to investigate the dynamic response of cement mortar mixed with GO. They found an increase in dynamic factor, and compressive and splitting tensile strengths in the samples with GO.

Based on the above literature review, even though there are a number of studies investigating the ability of GO in enhancing properties of cement material under high rates of loading, none have carried out tests with the actual explosive materials like Trinitrotoluene (TNT). This research aims to investigate the effect of GO on the blast resistance of FRC using TNT detonated under non-contact conditions. Four types of specimens were prepared, plain mortar (M), mortar mixed with graphene (MG), fiber reinforced mortar (FRM), and FRM mixed with GO (FRMG). The blast loading test was carried out under a non-contact TNT detonating condition. The investigation also included assessing basic mechanical properties such as compressive and flexural strength, and also microstructure using SEM and XRD. The results were analyzed and discussed in terms of failure pattern and level of protection due to blast resistance.

2. Experimental procedure

2.1 Materials

Materials used in this study consisted of Portland cement (ASTM C315), fine aggregate from local river sand with a particle size of 1.19-0.30 mm and size distribution as shown in Figure 1, clean tap water, and steel fiber (hooked-end type) with properties given in Table 1.

The GO was manufactured and produced at the Smart Materials Research and Innovation Unit (SMRIU) at King Mongkut's Institute of Technology Ladkrabang (KMITL) [65]. To prepare the GO solution, the oxidizing graphite was dissolved with a strong acid and oxidizing agent by the modified Hummer's method [66]. In the synthesizing process, the $KMnO_4$ and graphite powder were mixed in a beaker and cooled to 0°C for 10 min. Then, the H_2SO_4 was added while the temperature was maintained at below 15°C. Next, the distilled water was slowly added and stirred, and the temperature was slowly increased up to 95°C over a 60-minute time frame. After the chemical reaction completed, the distilled and H_2O_2 solution was added until the solution color changed to yellow-brown. Centrifugation was used to separate the GO nanosheets and sulphate was removed by washing it with HCl solution. In the purifying process, the GO nanosheets were filtered and washed several times with the distilled water until the pH level reached 7. The GO nanosheets obtained after purification were dried in an oven at 65°C for 24 hours. Before mixing with the mortar, the GO nanosheets powder was dispersed in distilled water with ultrasonication and centrifugation for 90 minutes until the GO solution was uniformly suspended in the solution. The properties of the GO solution are shown in Table 2.

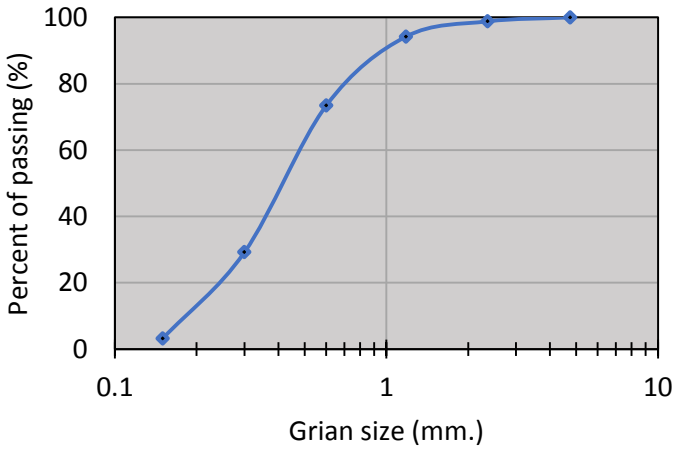

Figure 1. Grain size distribution of sand

Table 1. Properties of steel fiber

Properties	Unit	Description	Appearance
Material	-	Steel	
Type	-	Hooked-end	
Length	mm	35	
Diameter	mm	0.55	
Aspect ratio	-	65	
Elastic modulus	MPa	200,000	
Tensile strength	MPa	1,345	
Strain at ultimate strength	%	0.8	

Table 2. GO solution properties

Name	Graphene oxide solution (GO)
Type	Aqueous suspension
Thickness	Equal to Monolayer sheets of carbon (~0.34nm)
Color	Brown to very dark black
Dispersibility	Polar solvents (DI water)
Concentration	10 mg/mL
Specific surface area (BET surface area)	100-200 m^2/ g
Particle size (electron diffraction)	4-6 µm
Characteristics	High mechanical strength and flexibility, dielectric/non-conductivity.

2.2 Mix proportions and specimen preparation

Mix proportions of plain and FRM are shown in Table 3. The water/cement ratio and cement/sand ratio are set at 0.40 and 1:2.75, respectively. Previous research [17], [20][23] [67] indicated that the addition of 2% of steel fibers by volume effectively improved the mechanical properties of cement materials under impact penetration loading. Thus, the mix proportion of FRC in this study was set at 2% by volume. For the ratio of GO solution, evidence from literature recommended GO content not exceeding 0.1% by weight of cement [66][68]. Thus, the amount of GO was set at 0%, 0.025%, 0.050%, 0.075% and 0.100% by weight of cement.

The specimen preparation process began with dry mixing cement and sand for 2 minutes. The liquid part (clean water and GO solution) was mixed together prior to adding to the dry mix. For uniformly dispersed GO, the mixing time was continued for about 3 minutes for all specimen types until the GO was fully dispersed in the fresh mortar. In cases of FRM, the steel fiber was added to the fresh mortar by dividing the fibers into 3 parts. Each part of fiber was distributed to the mixer and mixed continuously for 1 min. The fresh mortar was then cast into steel molds by dividing into 3 layers, compacted on a vibration table for 1 minute, and wrapped in plastic sheeting overnight. After 24 hours, the specimens were demolded and cured under water for 28 days.

Table 3. Mix proportion

Designation	Description	GO (% by weight of cement)	Steel fiber (% by volume)	Cement	Water	Sand
				(kg/m^3)		
M	Plain mortar	0	0	580	230	1600
25MG	Plain mortar + GO	0.025				
50MG		0.050				
75MG		0.075				

100MG		0.100				
FRM	Fiber reinforced mortar	0	2			
25FRMG	Fiber reinforced mortar + GO	0.025				
50FRMG		0.050				
75FRMG		0.075				
100FRMG		0.100				

2.3 Experimental series

The experiment series is divided into 2 parts: 1) Physical and mechanical properties (setting time, flow test, compressive strength, and flexural strength), and 2) Blast loading test on the selected mix proportions. In addition, the change in microstructure due to the addition of GO was also investigated by using scanning electron microscopy (SEM) and X-ray diffraction (XRD).

2.3.1 Setting time and flow test

Both setting time and flow are important parameters used in determining the workability of graphene mortar. The setting time was carried out in accordance with the ASTM C807 standard using Vicat apparatus [69]. To begin a test, fresh mortar was poured in a testing mold, a Vicat needle was placed on the top surface and then released. The depth of penetration was observed and recorded together with the corresponding time. Both initial and final setting times for each mortar type were recorded.

For the flow test, the test was performed following the ASTM C230 standard using a flow table [70]. The fresh mortar was put into a reverse cone mold and compacted in 2 layers with a tamping rod 20 times/layer. The mold was then lifted slowly and vertically to allow the mortar to flow freely. The flow table was then raised and dropped in the vertical direction 25 times in 15 seconds. Finally, the flow diameter was measured in four perpendicular directions and used in calculating the average value.

2.3.2 Compressive and Flexural strength

A compressive strength test was carried out according to ASTM C39 [71] using cylindrical shaped specimens with a diameter of 100 mm and height of 200 mm. The rate of loading was controlled at 0.25±0.05 MPa/s. For the flexural strength, the specimens were cast in a prism shape with dimensions of 100 x 100 x 350 mm, in accordance with ASTM C1609 [72]. The rate of loading for the flexural test was set at 0.05 mm/min with a third-point loading pattern.

2.3.3 Blast loading test

Using the results from 2.3.2, the mix proportion with the highest compressive and flexural strengths was selected for the blasting test. The specimens were prepared in a panel form with dimensions of 500 mm x 1000 mm and thickness of 60 mm. The panel was reinforced with 6 mm-diameter round steel bars with 200 mm spacing as shown in Figure 2. To setup a test, a panel was placed and secured on the steel support (Figure 3), an explosive material (Trinitrotoluene, TNT) weighing 230 g (0.50 lb) was placed on temporary plastic supports with three different vertical standoff distances of 340, 400, and 460 mm (equivalent to blast incident pressure of 4090, 3094, and 2392 kPa, respectively). The antenna, used for measuring the deflection of the panel during the blast event, was securely installed at the bottom of the slab. Before igniting the TNT, the surrounding area was cleared and all personnel were relocated behind the bunker. An electrical detonator (electric blasting cap) was connected to the TNT and ignited using a 12V battery. After the explosion, the damage to the panel, permanent deflection, and maximum deflection were recorded and analyzed [73].

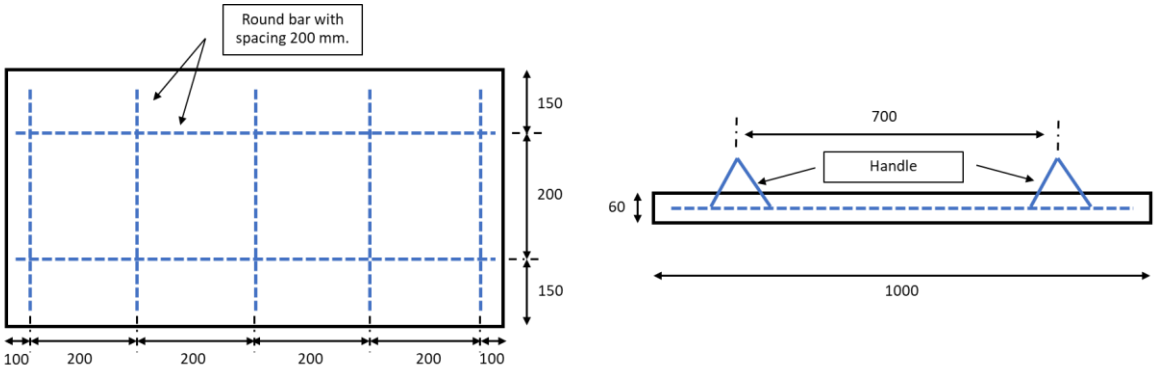

Figure 2. Steel reinforcement of specimen (unit in mm)

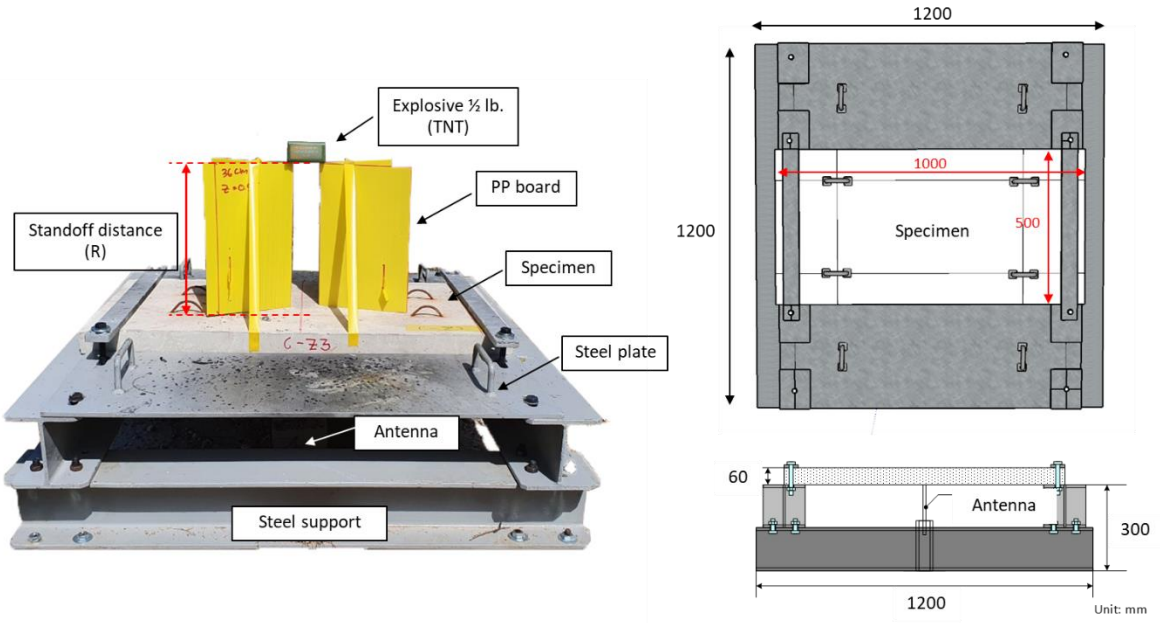

Figure 3. Blast impaction test setup (unit in mm)

4. Results and discussions

4.1 Physical and mechanical properties

4.1.1 Flowability and time of setting

The flow diameter was found to decrease with increasing GO content in both MG and FRMG, as shown in Figure 4. Comparing between FRMG and MG at the same GO content, the FRMG exhibited smaller flow diameter than MG because the existence of fibers interfered with workability of fresh mortar led to the decrease in flow diameter. For effect of GO on plain mortar and FRM, the flow diameter decreased by about 9% and 16% compared with non-GO mortar and FRM respectively. Similar findings were also reported [74]-[76], in that the addition of GO in the mortar lead to a decrease in workability of up to 27% due to the high specific surface area. This is because the addition of GO increases the water requirement of the mix which led to the decrease in free water available to mobilize the fresh mortar. In addition, the hydrophilic functional group and agglomeration of GO trapped the free water in the fresh cement matrix and reduced workability [77]-[80].

For the setting time, the addition of GO led to a slight decrease in initial and final setting times for both MG and FRMG (Figure 5). Wang [81] found that the addition of GO can accelerate the early stage of the hydration reaction due to the filling and nucleation effect of nanoparticles. The addition of high specific surface area materials like GO also caused difficulty in achieving a uniform dispersion in the cement matrix [62]. Comparing between MG and FRMG, the setting time of FRMG was found to almost identical to that of MG (Figure 5a).

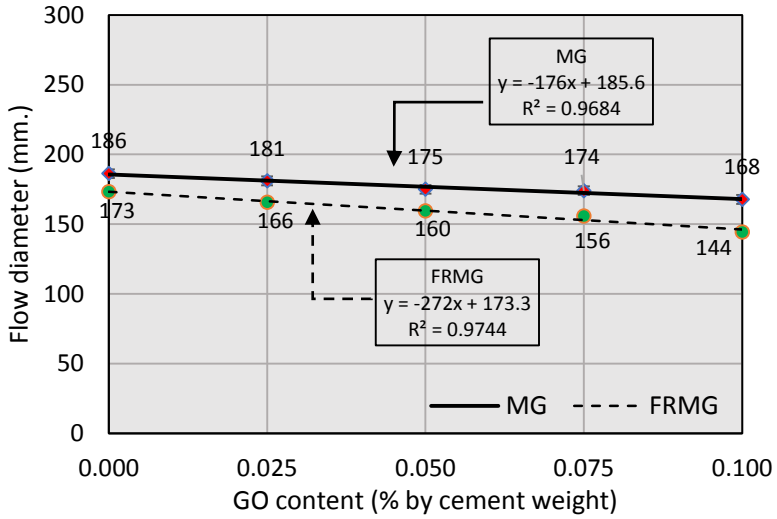

Figure 4. Flow diameter

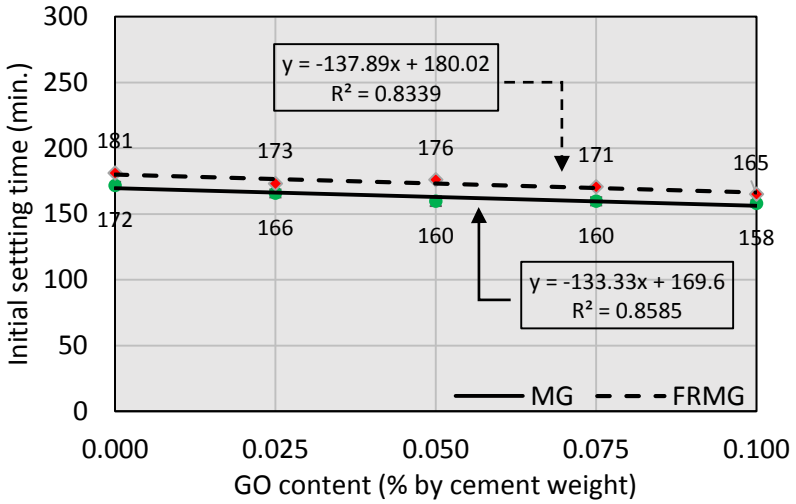

(a) Initial setting time

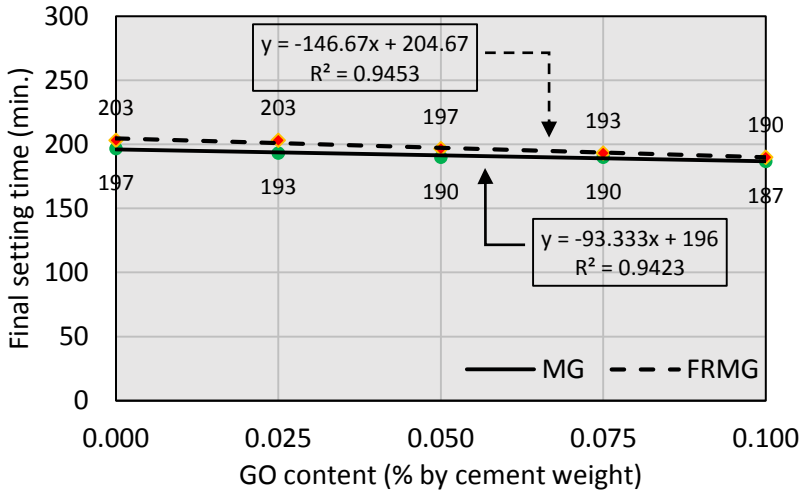

(b) Final setting time

Figure 5. Setting time

4.1.2 Compressive and flexural strength

The failure pattern of MG and FRMG under the compressive and flexural tests are shown in Figures 6 and 7. Under both compression and flexural loads, the plain mortar (M) specimens were found to fail in a brittle failure mode with large cracks running and propagating through the specimen's thickness. Although GO has excellent flexibility, the addition of GO provides no improvement in the ductility of MG as it failed under brittle mode similar to that of plain mortar (M). For FRM and FRMG, the ductile failure patterns were characterized by large numbers of small- and micro-cracks at the outer surface. This was due to the effect of the steel fibers bridging over the cracks, slowing down crack propagation, and preventing the specimen's disintegration.

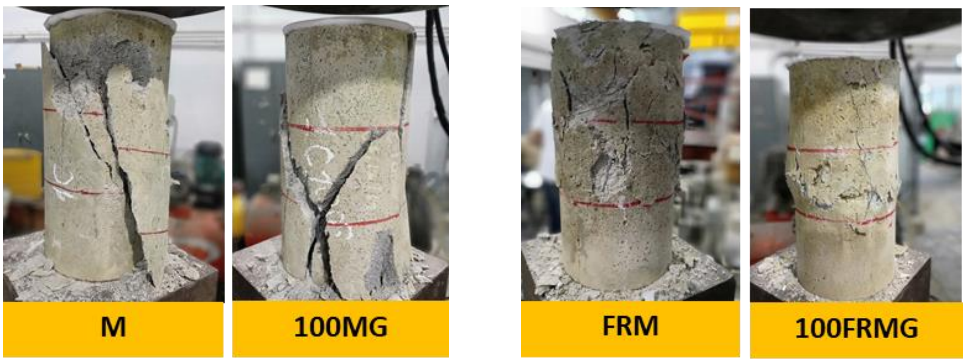

(a) (b)

Figure 6. Compression failure patterns: (a) brittle and (b) ductile modes

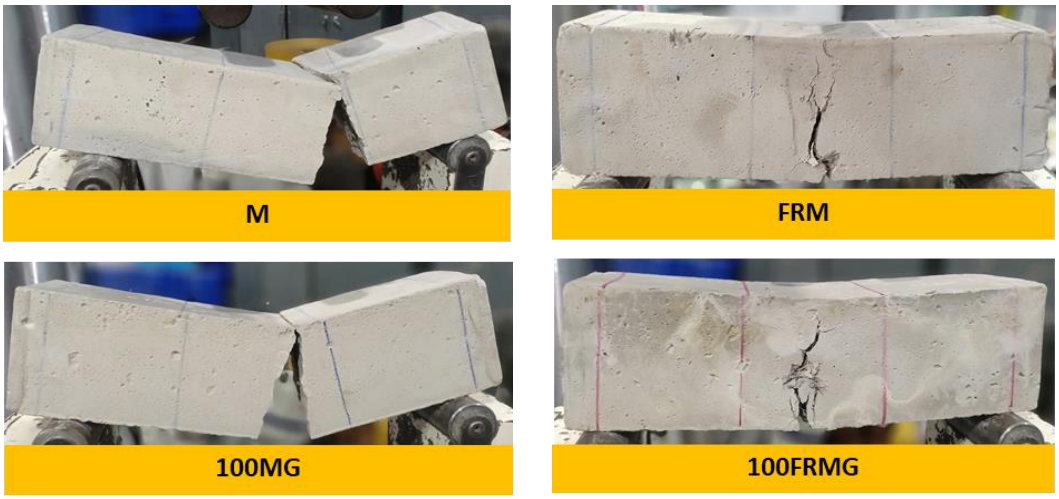

(a) (b)

Figure 7. Flexural failure patterns: (a) brittle and (b) ductile

The effects of GO on compressive and flexural strength are shown in Figures 8 and 9. For both loading types, the optimum GO content was observed to be 0.025%. The highest increase in compressive and flexural strength of 8% and 7% was observed in 25MG. This contributed to the filling effect and the improvement in bonding between the GO and mortar matrix [81][82].

On the other hand, the increase in GO dosage over the optimum content (0.025%) led to a decrease in strength. This was due to an increase in specific surface area from adding GO nanoparticles which caused difficulties in mixing and obtaining good compaction. Similarly, Qureshi et al. [83] found that 0.02% of graphene by cement weight was optimal to give the maximum compressive and flexural strengths, and if the addition of graphene exceeded 0.02%, the strength also decreased gradually.

In the case of FRMG, regardless of the GO content, the compressive strength of FRMG was slightly lower than MG in all cases. This was because large numbers of fibers (at high content of 2%)

lowered the workability which caused poor compaction and high porosity [84]. The optimum GO content for the FRMG was found to be similar to that of MG which was at 0.025%.

In the case of flexural strength, the results were the opposite of the compressive strength. The flexural strength of FRM and FRMG was higher than that of M and MG regardless of the GO content. This was due to the effect of fiber alignment which were mostly parallel to the stress plane when subjected to flexural loading. Niş et al. [85] reported similarly that the fibers were more aligned and oriented along the casting direction in the specimens with thinner sections than the specimens with deep sections.

Comparing between FRMG, the addition of GO at 0.025% also yielded the highest increase in the flexural strength by about 8.22 %. This was due to better bonding between the fiber and cement matrix as recently reported by Chindaprasirt et al. [46].

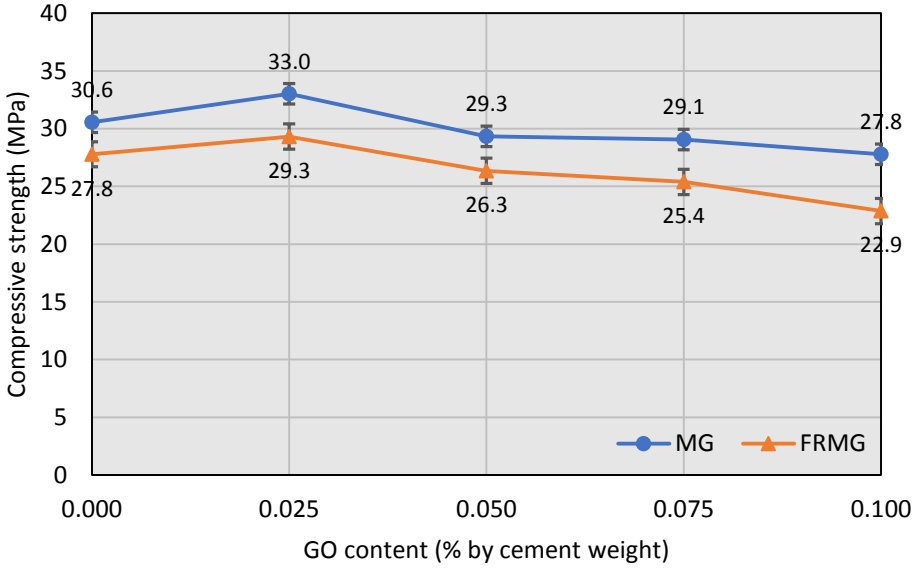

Figure 8. Compressive strength

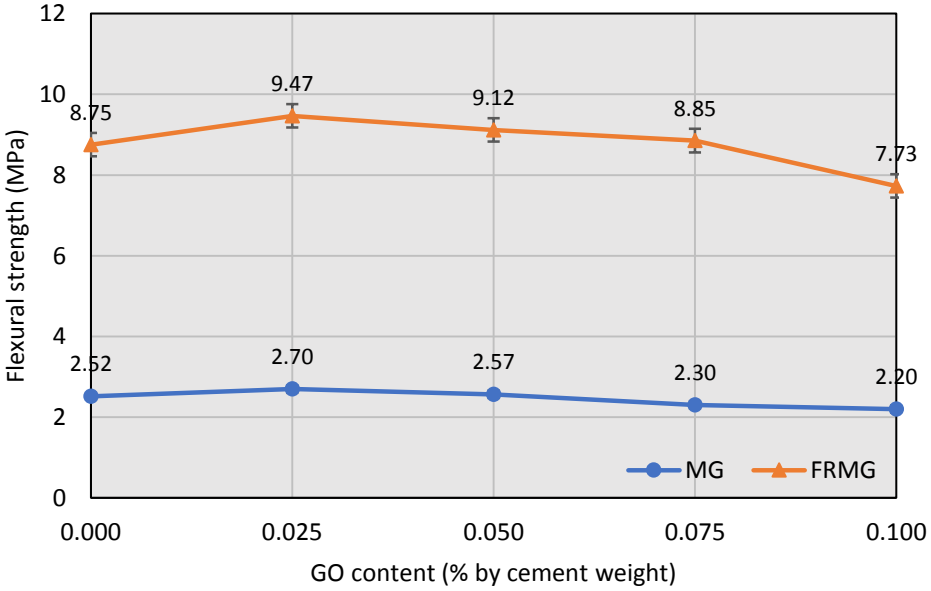

Figure 9. Flexural strength

4.1.3 Microstructure

To study the microstructure and element composition of the mortar with added GO, Scanning Electron Microscope (SEM) and X-ray Diffractometer (XRD) analyses were carried out. The SEM results in Figure 10 show that the addition of GO nanoparticles reduced the porosity of the mortar matrix due to the nano-filter effect [86][88]. Wang et al. [89] showed that the addition of graphene in cement composite can enhance the mechanical properties because nanofibers created crack bridge resistance.

As mentioned earlier, the addition of GO at proportions higher than 0.025% of cement weight led to strength decreases due to the difficulty in mixing and compaction. This can be supported by the results from the SEM images in Figure 10 which showed an increasing number of large voids in the mortar matrix when increasing the GO content higher than 0.025%.

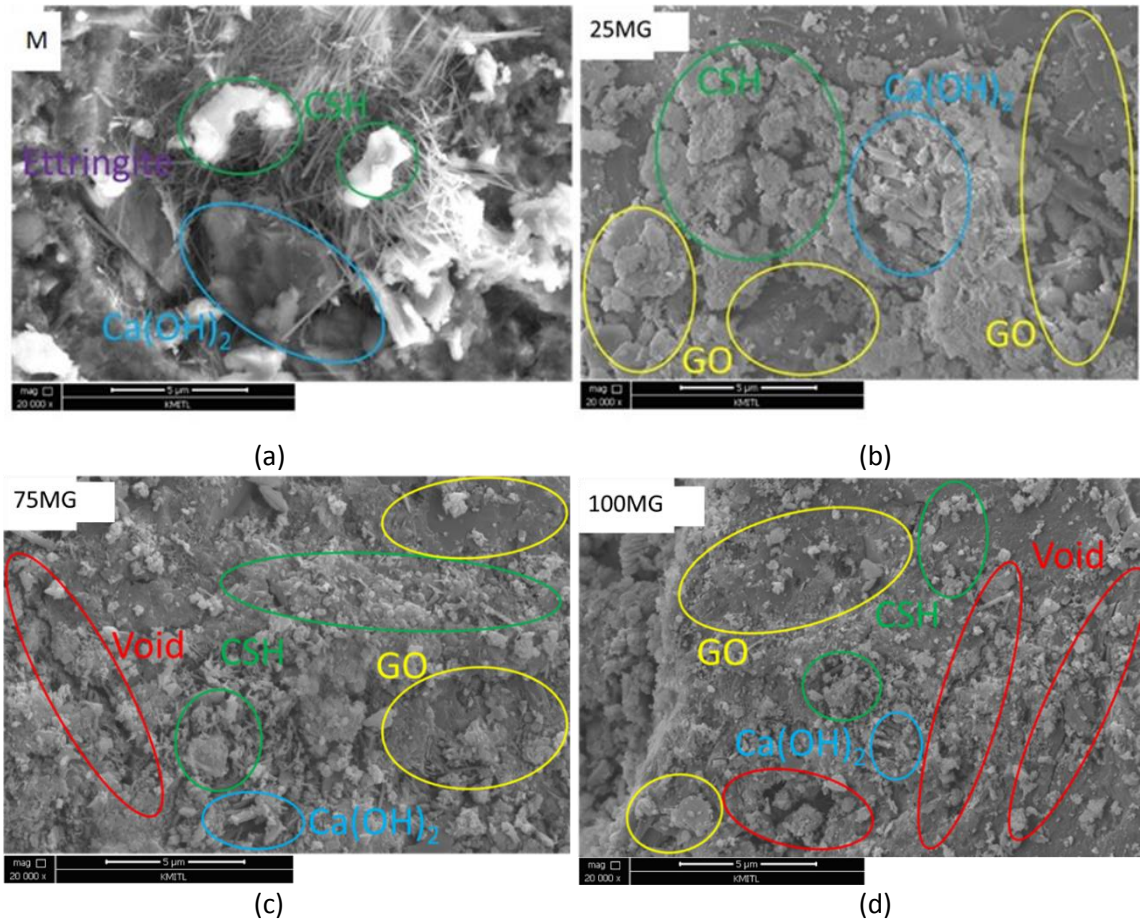

Figure 10. The SEM of mortar mixed with graphene oxide (a) M, (b) 25MG, (c) 75MG, (d) 100MG

The XRD results of mortar incorporated with GO at different dosages are shown in Figure 11. Generally, the hydration products of cement with portlandite (CH), ettringite, dicalcium silicate (C_2S) and tricalcium silicate (C_3S) were detected in mortar with GO dosages. As the XRD results show, the intensity of the peak for the CH phase at position 34.2°, 47.1° and 50.1° increased with increasing GO content indicating the ability of GO to improve cement hydration reaction [66] [83], [90]-[92]. With the increase of hydration reaction, the C_2S and C_3S phases at position 29.5° increased due to the precipitation of CH crystallites [93]. The major peak of quartz at 2-Theta of 26.7° was found in every GO dosage, relating to the mix proportion of sand [88].

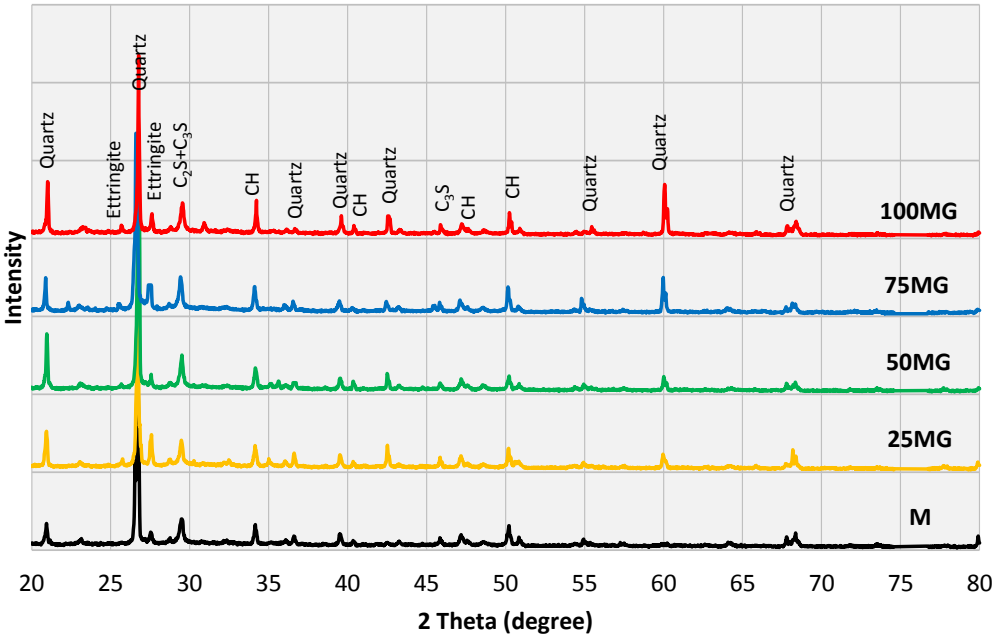

Figure 11. XRD pattern of MG

4.2 Blast loading test

Using the results obtained from 4.1.2, the optimum GO content of 0.025% by weight of cement was concluded for both MG and FRMG. Therefore, it was selected for the blast loading test. The test was performed on plain mortar (M), FRM and 25FRMG to investigate the effect of GO on enhancing blast resistance. The results were discussed in terms of failure mode and maximum deflection that occurred during the blast event.

4.2.1 Damage patterns

The damage patterns observed in the blast loading test were found to be strongly affected by the blasting incident pressure (i.e., standoff distance of the TNT) and the specimen types. The damage pattern can be divided into 3 patterns: complete flexural failure, flexural cracking, and no major damage with microcracking, as shown in Figures 12-14 and summarized in Table 4.

For the complete flexural failure mode, a large crack running through the panel's thickness was visibly observed on both the top and bottom surfaces. The failure is caused by a single crack propagating from the bottom surface across the thickness to the top. The burn marks that appeared on the top surface were a direct result of TNT exposure. The bottom surface suffered a large flexural crack. This failure pattern was found in plain mortar (M) panels subjected to TNT at every standoff distance (340, 400, and 460 mm) due to the brittleness and poor explosion resistance of the M specimens. In the case of FRM panels, this failure mode was found when the TNT was placed at the standoff distance of 340 mm which was the nearest distance and produced the strongest incident pressure. Even though the fibers were able to enhance blast resistance, they cannot prevent a complete flexural failure from occurring at the standoff distance of 340 mm (incident pressure of 4093 kPa).

The second failure mode was flexural cracking. In this mode, a visible crack was observed at the bottom surface of the panel around and outside the blasting region, and there was no sign of cracks at the top surface. This failure pattern was observed in both the FRM and FRMG which indicated the ability of the fibers to enhance explosive resistance and prevent complete failure from occurring. This mode was observed in FRM and 25FRMG at the standoff distance of 400 mm. At the standoff distance of 340 mm, while the FRM specimen suffered a complete flexural failure mode, the 25FRMG only showed flexural cracking mode. For 25FRMG to show a less severe failure mode at the highest incident

pressure of 4093 kPa (or standoff distance of 340 mm) demonstrates the ability of GO to supplement the blast resistance of FRM and prevent a complete flexural failure mode from occurring. Mindess [94] and Lai [95] indicated that the addition of steel fibers improved the blast resistance of mortar because of the fibers' ability to restrain cracks, prevent catastrophic failure, and minimize flying fragments from the impact load and bending fracture [8][96][99].

With the standoff distance increased to 460 mm, no major damage with microcracking failure mode was observed in both FRM and 25FRMG. Burn marks resulting from direct exposure to the blast loading were observed on the top surface. At the bottom surface, small microcracks were visually observed. Since there is no evidence of cracks at the side view photo (Figure 14), this indicated that these cracks only occurred at the surface but did not propagate through the thickness.

In addition, the ability of the fibers to enhance explosive resistance was partly due to the lesser explosive pressure and the longest standoff distance of 460 mm.

It must be noted here that, in this study, there was no spalling of mortar fragments found in any specimens. This was due to the nature of non-contact explosions. Unlike the contact explosion configuration where the failure mode is often accompanied by perforation, spalling, and flying debris [100]-[104], the non-contact explosion type is less severe.

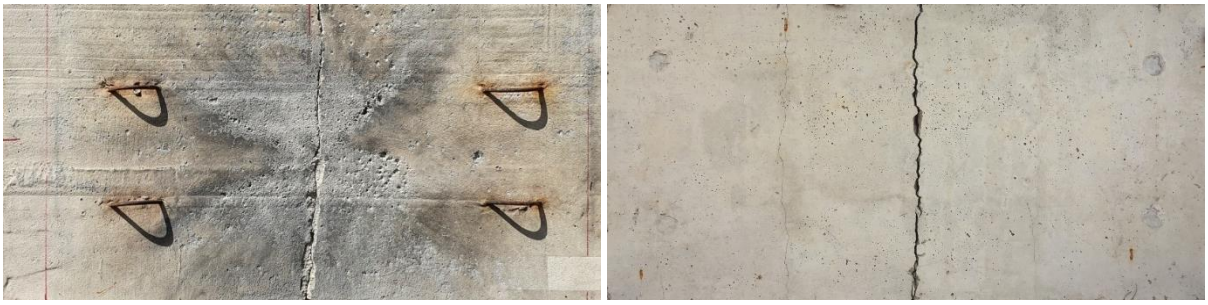

a) Top b) Bottom

c) Side

Figure 12. Complete flexural failure pattern

a) Top b) Bottom

c) Side

Figure 13. Flexural cracking pattern

a) Top b) Bottom

c) Side

Figure 14. No major damage with microcracking pattern

Table 4. Damage patterns

Blast cases	Type	Standoff distance (mm)	Damage pattern
M-R340	Plain mortar (M)	340	Complete flexural failure
M-R400		400	Complete flexural failure
M-R460		460	Complete flexural failure
FRM-R340	Fiber reinforced mortar (FRM)	340	Complete flexural failure
FRM-R400		400	Flexural cracking
FRM-R460		460	No major damage with microcracking
25FRMG-R340	Fiber reinforced mortar with 0.025%wt GO (25FRMG)	340	Flexural cracking
25FRMG-R400		400	Flexural cracking
25FRMG-R460		460	No major damage with microcracking

4.2.2 Maximum and permanent deflections

Results on the maximum and permanent deflections are shown in Figure 15. In general, the typical response of a panel subjected to blast loading includes a downward bending of the panel (to the maximum deflection) during the blasting event and a partial rebound of the panel at the end of the event which leaves behind a permanent deflection. On the effect of standoff distance, both maximum and permanent deflections were found to decrease with the increasing standoff distance. This is clearly because of the decrease in blast incident pressure (from 4090 to 2392 kPa) with the increasing standoff distance of the TNT away from the target (from 340 to 460 mm).

Comparing between M, FRM, and 25FRMG at the same blast incident pressure, both maximum and permanent deflections was highest in M, followed by FRM and finally 25FRMG. This showed that steel fibers were able to increase the blast loading resistance and specimen stiffness and reduce deflections. As for the effect of GO, comparing between FRM and 25FRMG, the maximum deflection was found to be in a similar range when subjected to the same incident pressure. However, in the case

of permanent deflection, 25FRMG exhibited lower permanent deflection than FRM. This is perhaps due to the flexibility of GO and the enhanced bond strength between steel fibers and GO material which allowed the panels to rebound back more effectively and limited the deflection of the specimen, resulting in less permanent deflection[46].

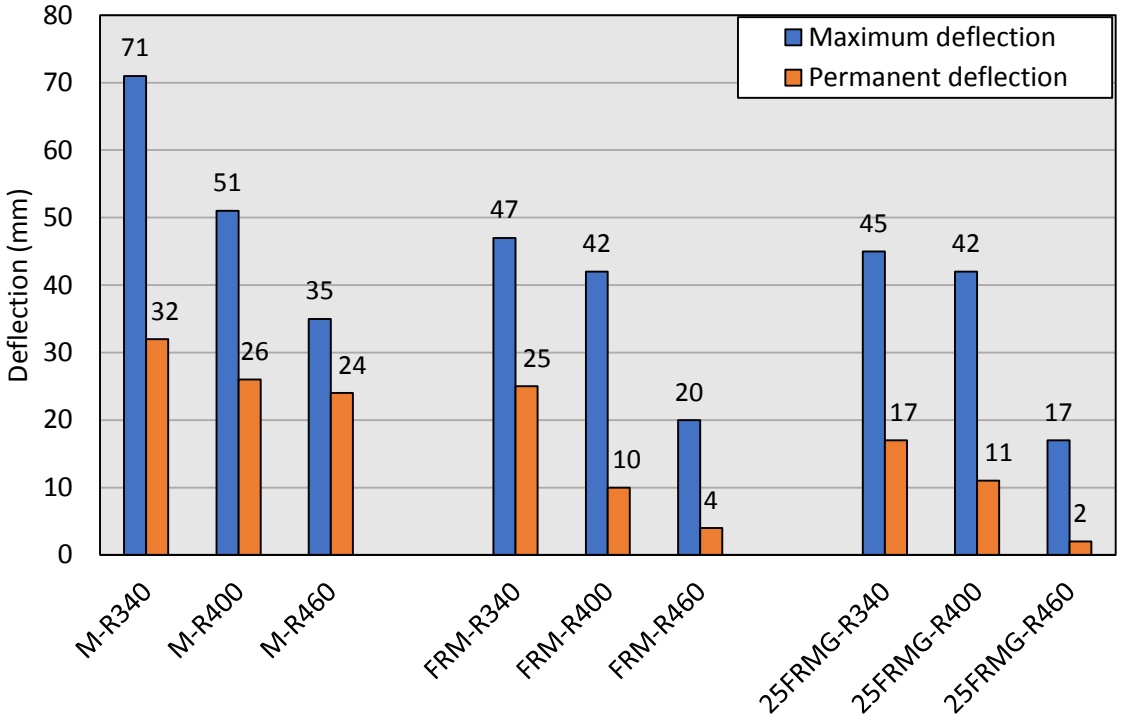

Figure 15. Deflection

5. Conclusions

In this study, the properties and blast resistance of steel fiber reinforced mortar incorporated with GO at 0-0.1% were investigated. The optimum dosage of graphene oxide was determined and blast loading test was carried out using TNT detonated under non-contact condition. Based on the obtained experimental results, the conclusion can be summarized as follows:

- The workability and setting time of mortar decreases with increasing graphene oxide dosages due to the increase in specific surface area and the increase in hydration reaction rate from the addition of GO nanoparticles.
- The optimum GO content of 0.025% by cement weight was observed in this study for both MG and FRMG. With GO dosages over 0.025%, the strength was found to decrease gradually.
- The results from both SEM images and XRD supported the findings that the increase in strength was due to the increase in crystallization of portlandite in the cement hydration reaction from the addition of GO.
- The results of the blast loading test demonstrated 3 damage patterns: complete flexural failure, flexural cracking and no major damage with microcracking. The level of damage depended strongly on the standoff distance and specimen type. At the closest standoff distance (highest explosive pressure), both M and FRM failed under complete flexural failure mode, while FRMG suffered less severe damage (flexural cracking). This indicated that GO was able to enhance the blast loading of FRM.
- As for the deflection, the FRMG was found to exhibit less maximum and permanent deflection than both M and FRM. The smaller permanent deflection showed the flexibility of GO and enhanced bond strength between fiber and mortar matrix which allowed the FRMG to rebound more effectively, resulting in less permanent deflection.

6. Acknowledgements

The authors would like to dedicate this work to Lt. Col. Amornthep Somrat for his strong devotion to this research, he will always be in our memories.

The research was funded by the Armament Research Fellowship Program for Enhancement of Armed Forces and National Defense Thailand. The authors would like to acknowledge support from Smart Materials Research and Innovation Unit, KMITL for providing the graphene oxide, Chulachomklao Royal Military Academy for supporting detonation, and also from King Mongkut's University of Technology North Bangkok and Rajamangala University of Technology Phra Nakhon for laboratory support. The last author would like to acknowledge funding from the National Science, Research and Innovation Fund (NSRF) and King Mongkut's University of Technology North Bangkok (KMUTNB) under the contract no. KMUTNB-FF-66-02. Special thank is also to Ruth Saint for proofreading the manuscript.

7. References

[1] P. Sukontasukkul, "Tensile behaviour of hybrid fibre-reinforced concrete," Advances in Cement Research, vol. 16, no. 3, pp. 115-122, 2004. https://doi.org/10.1680/adcr.2004.16.3.115

[2] P. Jamsawang, T. Suansomjeen, P. Sukontasukkul, P. Jongpradist and D. T.Bergado, "Comparative flexural performance of compacted cement-fiber-sand," Geotextiles and Geomembranes, vol. 46, no. 4, pp. 414-425, 2018. https://doi.org/10.1016/j.geotexmem.2018.03.008

[3] C. Chaikaew, P. Sukontasukkul, U. Chaisakulkiet, V. Sata and P. Chindaprasirt, "Properties of Concrete Pedestrian Blocks Containing Crumb Rubber from Recycle Waste Tyres Reinforced with Steel Fibres," Case Studies in Construction Materials, vol. 11, e00304, 2019. https://doi.org/10.1016/j.cscm.2019.e00304

[4] P. Sukontasukkul, P. Chindaprasirt, P. Pongsopha, T. Phoo-ngernkham, W. Tangchirapat and N. Banthia, "Effect of fly ash/silica fume ratio and curing condition on mechanical properties of fiber-reinforced geopolymer," Journal of Sustainable Cement-Based Materials, vol. 9, no. 4, pp. 1-15, 2020. https://doi.org/10.1080/21650373.2019.1709999

[5] P. Nuaklong, A. Wongsa, K. Boonserm, C. Ngohpok, P. Jongvivatsakul, V. Sata, P. Sukontasukku and P. Chindaprasirt, "Enhancement of mechanical properties of fly ash geopolymer containing fine recycled concrete aggregate with micro carbon fibe," Journal of Building Engineering, vol. 41, 102403, 2021. https://doi.org/10.1016/j.jobe.2021.102403

[6] D.-Y. Yoo, J. Je, H.-J. Choi and P. Sukontasukkul, "Influence of embedment length on the pullout behavior of steel fibers from ultra-high-performance concrete," Materials Letters, vol. 276, 128233, 2020. https://doi.org/10.1016/j.matlet.2020.128233

[7] P. Sukontasukkul, U. Chaisakulkiet, P. Jamsawang, S. Horpibulsuk, C. Jaturapitakkul and P. Chindaprasirt, "Case investigation on application of steel fibers in roller compacted concrete pavement in Thailand," Case Studies in Construction Materials, vol. 11, e00271, 2019. https://doi.org/10.1016/j.cscm.2019.e00271

[8] M. Sappakittipakorn, P. Sukontasukkul, H. Higashiyama and PrinyaChindaprasirt, "Properties of Hooked End Steel Fiber Reinforced Acrylic Modified Concrete," Construction and Building Materials, vol. 186, pp. 1247-1255, 2018. https://doi.org/10.1016/j.conbuildmat.2018.08.055

[9] R. Wongruk, S. Songpiriyakij, P. Sukontasukkul and P. Chindaprasirt, "Properties of Steel Fiber Reinforced Geopolymer," Key Engineering Materials, vol. 659, pp. 143-148, 2015. https://doi.org/10.4028/www.scientific.net/KEM.659.143

[10] M. Jamnongwong, K. Krairan, H. Poorahong, P. Sukontasukkul and P. Jamsawang, "Effect of fiber types on flexural performance of compacted cement-fiber-sand," Suranaree Journal of Science & Technology , vol. 26, no. 4, pp. 421-428, 2019.

[11] P. Sukontasukkul, S. Jamnam, M. Sappakittipakorn, K. Fujikake and P. Chindaprasirt, "Residual flexural behavior of fiber reinforced concrete after heating," Materials and Structures, vol. 51, p. 98, 2018. https://doi.org/10.1617/s11527-018-1210-3

[12] W. Wongprachum, M. Sappakittipakorn, P. Sukontasukkul, P. Chindaprasirt and N. Banthia, "Resistance to sulfate attack and underwater abrasion of fiber reinforced cement mortar," Construction and Building Materials, vol. 189, pp. 686-694, 2018. https://doi.org/10.1016/j.conbuildmat.2018.09.043

[13] T. N. H. Tran, A. Puttiwongrak, P. Pongsopha, D. Intarabut, P. Jamsawang and P. Sukontasukkul, "Microparticle filtration ability of pervious concrete mixed with recycled synthetic fibers," Construction and Building Materials, vol. 270, p. 121807, 2021. https://doi.org/10.1016/j.conbuildmat.2020.121807

[14] D.-Y. Yoo and N. Banthia, "Mechanical properties of ultra-high-performance fiber-reinforced concrete: A review," Cement and Concrete Composites, vol. 73, pp. 267-280, 2016. https://doi.org/10.1016/j.cemconcomp.2016.08.001

[15] D.-Y. Yoo and N. Banthia, "Impact resistance of fiber-reinforced concrete – A review," Cement and Concrete Composites, vol. 104, p. 103389, 2019. https://doi.org/10.1016/j.cemconcomp.2019.103389.

[16] P. Sukontasukkul, S. Mindess, N. Banthia and T. Mikami, "Impact resistance of laterally confined fibre reinforced concrete plates," Materials and Structures, vol. 34, no. 10, pp. 612-618, 2001. https://doi.org/10.1007/BF02482128

[17] P. Sukontasukkul, S. Jamnam, K. Rodsin and N. Banthia, "Use of rubberized concrete as a cushion layer in bulletproof fiber reinforced concrete panels," Construction and Building Materials, vol. 41, pp. 801-811, 2013. https://doi.org/10.1016/j.conbuildmat.2012.12.068

[18] P. Sukontasukkul and S. Mindess, "The shear fracture of concrete under impact loading using end confined beams," Materials and Structures, vol. 36, no. 6, pp. 372-378, 2003. https://doi.org/10.1007/BF02481062

[19] P. Sukontasukkul, S. Jamnam, M. Sappakittipakorn and N. Banthia, "Preliminary study on bullet resistance of double-layer concrete panel made of rubberized and steel fiber reinforced concrete," Materials and Structures, vol. 47, pp. 1-2, 2012. https://doi.org/10.1617/s11527-013-0049-x

[20] B. Maho, P. Sukontasukkul, S. Jamnam, E. Yamaguchi, K. Fujikake and N. Banthia, "Effect of rubber insertion on impact behavior of multilayer steel fiber reinforced concrete bulletproof panel," Construction and Building Materials, vol. 216, pp. 476-484, 2019. https://doi.org/10.1016/j.conbuildmat.2019.04.243

[21] P. Sukontasukkul, S. Mindess and N. Banthia, "Penetration resistance of hybrid fibre reinforced concrete under low velocity impact loading," in Annual Conference of the Canadian Society for Civil Engineering, Canada, 2002.

[22] B. Maho, S. Jamnam, P. Sukontasukkul, K. Fujikake and N. Banthia, "Preliminary Study on Multilayer Bulletproof Concrete Panel: Impact Energy Absorption and Failure Pattern of Fibre Reinforced Concrete, Para-Rubber and Styrofoam Sheets," Procedia Engineering, vol. 210, pp. 369-376, 2017. https://doi.org/10.1016/j.proeng.2017.11.090.

[23] S. Jamnam, B. Maho, A. Techaphatthanakon, Y. Sonoda, D. Y. Yoo and P. Sukontasukkul, "Steel fiber reinforced concrete panels subjected to impact projectiles with different caliber sizes and muzzle energies," Case Studies in Construction Materials, vol. 13, 2020. https://doi.org/10.1016/j.cscm.2020.e00360

[24] A. Niş, N. A. Eren, and A. Çevik, "Effects of recycled tyre rubber and steel fibre on the impact resistance of slag-based self-compacting alkali-activated concrete," Eur. J. Environ. Civ. Eng., vol. 0, no. 0, pp. 1–19, 2022, https://doi.org /10.1080/19648189.2022.2052967.

[25] A. Niş, N. A. Eren, and A. Çevik, "Effects of nanosilica and steel fibers on the impact resistance of slag based self-compacting alkali-activated concrete," Ceram. Int., vol. 47, no. 17, pp. 23905–23918, 2021, https://doi.org/10.1016/j.ceramint.2021.05.099.

[26] D.-Y. Yoo, N. Banthia and Y.-S. Yoon, "Impact Resistance of Reinforced Ultra-High-Performance Concrete Beams with Different Steel Fibers," ACI Structural Journal, vol. 114, no. 1, pp. 113-124, 2017. http://dx.doi.org/10.14359/51689430

[27] K. Neme, A. Nafady, S. Uddin and Y. B.Tola, "Application of nanotechnology in agriculture, postharvest loss reduction and food processing: food security implication and challenge," Heliyon, vol. 7, no. 12, e08539, 2021. https://doi.org/10.1016/j.heliyon.2021.e08539

[28] S. Bokka and A. Chowdhury, "Evolving Trends of Nanotechnology for Medical and Biomedical Applications: A Review," in Module in Materials Science and Materials Engineering, Elsevier, 2021. https://doi.org/10.1016/B978-0-12-820352-1.00098-5.

[29] V. Leso, L. Fontana and I. Iavicoli, "Biomedical nanotechnology: Occupational views," Nano Today, vol. 24, pp. 10-14, 2019. https://doi.org/10.1016/j.nantod.2018.11.002.

[30] A. P. Tom, "Nanotechnology for sustainable water treatment – A review," Materials Today: Proceedings, 2021. https://doi.org/10.1016/j.matpr.2021.05.629.

[31] S. A. Bha, F. Sher, M. Hameed, O. Bashir, R. Kumar, D.-V. N. Vo, P. Ahmad and E. C. Lima, "Sustainable nanotechnology based wastewater treatment strategies: achievements, challenges and future perspectives," Chemosphere, vol. 288 part 3, 2022. 132606. https://doi.org/10.1016/j.chemosphere.2021.132606.

[32] B. Maho, P. Sukontasukkul, G. Sua-Iam, M. Sappakittipakorn, D. Intarabut, C. Suksiripattanapong, P. Chindaprasirt and S. Limkatanyu, "Mechanical properties and electrical resistivity of multiwall carbon nanotubes incorporated into high calcium fly ash geopolymer," Case Studies in Construction Materials, vol. 15, 2021. e00785. https://doi.org/10.1016/j.cscm.2021.e00785.

[33] P. Nuaklong, N. Boonchoo, P. Jongvivatsakul, T. Charinpanitkul and P. Sukontasukkul, "Hybrid effect of carbon nanotubes and polypropylene fibers on mechanical properties and fire resistance of cement mortar," Construction and Building Materials, vol. 275, 122189, 2021.

[34] K. Loamrat, M. Sappakittipakorn and P. Sukontasukkul, "Electrical Resistivity of Cement-Based Sensors under a Sustained Load," Advanced Materials Research, Vols. 931-932, pp. 436-440, 2014.

[35] K. Loamrat, M. Sappakittipakorn and P. Sukontasukkul, "Application of Cement-Based Sensor on Compressive Strain Monitoring in Concrete Members," Advanced Materials Research, Vols. 931-932, pp. 446-450, 2014. https://doi.org/10.4028/www.scientific.net/AMR.931-932.446

[36] S. Dueramaea, W. Tangchirapat, P. Chindaprasirt, C. Jaturapitakkul and P. Sukontasukkul, "Autogenous and drying shrinkages of mortars and pore structure of pastes made with activated binder of calcium carbide residue and fly ash," Construction and Building Materials, vol. 230, 116962, 2020. https://doi.org/10.1016/j.conbuildmat.2019.116962

[37] S. Hanjitsuwan, B. Injorhor, T. Phoo-ngernkham, N. Damrongwiriyanupap, L.-Y. Li, P. Sukontasukkul and P. Chindaprasirt, "Drying shrinkage, strength and microstructure of alkali-activated high-calcium fly ash using FGD-gypsum and dolomite as expansive additive," Cement and Concrete Composites, vol. 114, 103760, 2020. https://doi.org/10.1016/j.cemconcomp.2020.103760

[38] S. Dueramae, W. Tangchirapat, P. Sukontasukkul, P. Chindaprasirtd and C. Jaturapitakkul, "Investigation of compressive strength and microstructures of activated cement free binder from fly ash - calcium carbide residue mixture," Journal of Materials Research and Technology, vol. 8, no. 5, pp. 4757-4765, 2019. https://doi.org/10.1016/j.jmrt.2019.08.022

[39] A. Wongsa, A. Siriwattanakarn, P. Nuaklong, V. Sata, P. Sukontasukkul and P. Chindaprasirt, "Use of recycled aggregates in pressed fly ash geopolymer concrete," Environmental Progress & Sustainable Energy, vol. 39, no. 2, e13327, 2019. https://doi.org/10.1002/ep.13327

[40] P. Sukontasukkul, N. Nontiyutsirikul, S. Songpiriyakij, K. Sakai and P. Chindaprasirt, "Use of phase change material to improve thermal properties of lightweight geopolymer panel," Materials and Structures, vol. 49, p. 4637–4645, 2016.

[41] P. Sukontasukkul, T. Sutthiphasilp, C. Wonchalerm and P. Chindaprasirt, "Improving thermal properties of exterior plastering mortars with phase change materials with different melting temperatures: paraffin and polyethylene glycol," Advances in Building Energy Research, vol. 13, no. 1, pp. 1-21, 2018.

[42] P. Sukontasukkul, E. Intawong, P. Preemanoch and P. Chindaprasirt, "Use of paraffin impregnated lightweight aggregates to improve thermal properties of concrete panels," Materials and Structures, vol. 49, pp. 1793-1803, 2016.

[43] P. Uthaichotirat, P. Sukontasukkul, P. Jitsangiam, Cherdsak, Suksiripattanapong, V. Sata and P. Chindaprasirt, "Thermal and sound properties of concrete mixed with high porous aggregates from manufacturing waste impregnated with phase change material," Journal of Building Engineering, vol. 29, 101111, 2020. https://doi.org/10.1016/j.jobe.2019.101111

[44] P. Sukontasukkul, T. Sangpet, M. Newlands, D.-Y. Yoo, W. Tangchirapat, S. Limkatanyu and P. Chindaprasirt, "Thermal storage properties of lightweight concrete incorporating phase change materials with different fusion points in hybrid form for high temperature applications," Heliyon, vol. 6, no. 9, e04863, 2020. https://doi.org/10.1016/j.heliyon.2020.e04863

[45] P. Pongsopha, P. Sukontasukkul, TanakornPhoo-ngernkham, T. Imjai, P. Jamsawang and P. Chindaprasirt, "Use of burnt clay aggregate as phase change material carrier to improve thermal properties of concrete panel," Case Studies in Construction Materials, vol. 11, e00242, 2019. https://doi.org/10.1016/j.cscm.2019.e00242.

[46] P. Chindaprasirt, P. Sukontasukkul, A. Techaphatthanakon, S. Kongtun, C. Ruttanapun, D.-Y. Yoo, W. Tangchirapat, S. Limkatanyu and N. Banthia, "Effect of graphene oxide on single fiber pullout behavior," Construction and Building Materials, vol. 280, 122539, 2021. https://doi.org/10.1016/j.conbuildmat.2021.122539

[47] D. Intarabut, P. Sukontasukkul, T. Phoo-Ngernkham, H. Zhang, D.-Y. Yoo, S. Limkatanyu and P. Chindaprasirt, "Influence of Graphene Oxide Nanoparticles on Bond-Slip Reponses between Fiber and Geopolymer Mortar," Nanomaterials, vol. 12, no. 6, p. 943, 2022. https://doi.org/10.3390/nano12060943.

[48] K. Tontiwattanakul, J. Sanguansin, V. Ratanavaraha, V. Sata, S. tLimkatanyu and P. Sukontasukkul, "Effect of viscoelastic polymer on damping properties of precast concrete panel," Heliyon, vol. 7, no. 5, e06967, 2021. https://doi.org/10.1016/j.heliyon.2021.e06967

[49] A. Çevik, R. Alzeebaree, G. Humur, A. Niş, and M. E. Gülşan, “Effect of nano-silica on the chemical durability and mechanical performance of fly ash based geopolymer concrete,” Ceram. Int., vol. 44, no. 11, pp. 12253–12264, 2018, https://doi.org/10.1016/j.ceramint.2018.04.009.

[50] M. E. Gülşan, R. Alzeebaree, A. A. Rasheed, A. Niş, and A. E. Kurtoğlu, “Development of fly ash/slag based self-compacting geopolymer concrete using nano-silica and steel fiber,” Constr. Build. Mater., vol. 211, pp. 271–283, 2019, https://doi.org/10.1016/j.conbuildmat.2019.03.228.

[51] N. A. Eren, R. Alzeebaree, A. Çevik, A. Niş, A. Mohammedameen, and M. E. Gülşan, “Fresh and hardened state performance of self-compacting slag based alkali activated concrete using nanosilica and steel fiber,” J. Compos. Mater., vol. 55, no. 28, pp. 4125–4139, 2021, https://doi.org /10.1177/00219983211032390.

[52] M. Raji, N. Zari, A. e. k. Qaiss and R. Bouhfid, "Chapter 1 - Chemical Preparation and Functionalization Techniques of Graphene and Graphene Oxide," in In Micro and Nano Technologies, Functionalized Graphene properties and its application, Elsevier, 2019, pp. 1-20. https://doi.org/10.1016/B978-0-12-814548-7.00001-5.

[53] B. SA, U. N, B. FA, I. M and S. S., "A review of functionalized graphene properties and its application," International Journal of Innovation Science and Research, vol. 17, 2015. 303e15
[54] W. Dong, W. Li, Y. Guo, K. Wang and D. Sheng, "Mechanical properties and piezoresistive performances of intrinsic graphene nanoplate/cement-based sensors subjected to impact load," Construction and Building Materials, vol. 327, 126978, 2022. https://doi.org/10.1016/j.conbuildmat.2022.126978.
[55] H. Du and S. D. Pang, "Dispersion and stability of graphene nanoplatelet in water and its influence on cement composites," Construction and Building Materials, vol. 167, pp. 403-413, 2018.
[56] G. Jing, Z. Ye, X. Lu and P. Hou, "Effect of graphene nanoplatelets on hydration behaviour of Portland cement by thermal analysis," Advances in Cement Research, vol. 29, no. 2, pp. 63-70, 2016.
[57] X. Li, Z. Lu, S. Chuah, W. Li, Y. Liu and W. Duan, "Effects of graphene oxide aggregates on hydration degree, sorptivity, and tensile splitting strength of cement paste," Composites Part A: Applied Science and Manufacturing, vol. 100, pp. 1-8, 2017
[58] J. An, M. McInnis, W. Chung and B. Nam, "Feasibility of using graphene oxide nanoflake (GONF) as additive of cement composite," Applied Sciences, vol. 8, p. 419, 2018.
[59] K. Gong, Z. Pan, A. Korayem, L. Qiu, D. Li and F. Collins, "Reinforcing effects of graphene oxide on portland cement paste," Journal of Materials in Civil Engineering, vol. 27, 2015. A4014010.
[60] Z. Pan, L. He, L. Qiu, A. Korayem, L. Gang, J. Zhu and F. Collins, "Mechanical properties and microstructure of a graphene oxide-cement composite," Cement and Concrete Composites, vol. 58, pp. 140-147, 2015.
[61] W. Long, Y. Cu, B. Xiao, Q. Zhang and F. Xing, "Micro-mechanical properties and multi-scaled pore structure of graphene oxide cement paste: Synergistic application of nanoindentation, X-ray computed tomography, and SEM-EDS analysis," Construction and Building Materials, vol. 179, pp. 661-674, 2018.
[62] Y. Lin and H. Du, "Graphene reinforced cement composites: A review.," Construction and Building Materials, vol. 265, 2020. 120312. https://doi.org/10.1016/j.conbuildmat.2020.120312
[63] J. Wang, S. Dong, X. Yu and B. Han, "Mechanical properties of graphene-reinforced reactive powder concrete at different strain rates," Journal of Materials Science, vol. 55, p. 3369–3387, 2020. https://doi.org/10.1007/s10853-019-04246-5
[64] C. Y. Li, S. J. Chen, W. G. Li, X. Y. Li, D. Ruan and W. H. Duan, "Dynamic increased reinforcing effect of graphene oxide on cementitious nanocomposite," Construction and Building Materials, vol. 206, pp. 694-702, 2019. https://doi.org/10.1016/j.conbuildmat.2019.02.001
[65] C. Phrompet, C. Sriwong and C. Ruttanapun, "Mechanical, dielectric, thermal and antibacterial properties of reduced graphene oxide (rGO)-nanosized C3AH6 cement nanocomposites for smart cement-based materials," *Composites Part B: Engineering,* vol. 175, 2019. https://doi.org/10.1016/j.compositesb.2019.107128
[66] L. Zhao, X. Guo, L. Song, Y. Song, G. Dai and J. Liu, "An intensive review on the role of graphene oxide in cement-based materials," *Construction and Building Materials,* vol. 241, 2020. https://doi.org/10.1016/j.conbuildmat.2019.117939
[67] R. Sovják, T. Vavřiník, J. Zatloukal, P. Máca, T. Mičunek and M. Frydrýn, "Resistance of slim UHPFRC targets to projectile impact using in-service bullets," *International Journal of Impact Engineering,* vol. 76, pp. 166-177, 2015. https://doi.org/10.1016/j.ijimpeng.2014.10.002
[68] Y. Lin and H. Du, "Graphene reinforced cement composites: A review.," Construction and Building Materials, vol. 265, 2020. 120312. https://doi.org/10.1016/j.conbuildmat.2020.120312
[69] A. C807-21, Standard Test Method for Time of Setting of Hydraulic Cement Mortar by Modified Vicat Needle, West Conshohocken, PA: ASTM International, 2021. www.astm.org

[70] ASTM C230 /. C230M-21, Standard Specification for Flow Table for Use in Tests of Hydraulic Cement, West Conshohocken, PA: ASTM International, 2021. www.astm.org
[71] ASTM C39/. C39M-21, Standard Test Method for Compressive Strength of Cylindrical Concrete Specimens, West Conshohocken, PA: ASTM International, 2021., www.astm.org
[72] ASTM C1609 /. C1609M-19a, Standard Test Method for Flexural Performance of Fiber-Reinforced Concrete (Using Beam With Third-Point Loading), West Conshohocken, PA: ASTM International, 2019 www.astm.org
[73] PDC-TR 06-08, "Single Degree of Freedom Blast Design Spreadsheet (SBEDS) Methodology," U.S. Army Corps of Engineers Protective Design Center Technical Report, 2008.
[74] L. Lu and D. Ouyang, "Properties of cement mortar and ultra-high strength concrete incorporating graphene oxide nanosheets," *Nanomaterials ,* vol. 7, no. 7, 2017. https://doi.org/10.3390/nano7070187
[75] W. J. Long, J. J. Wei, H. Ma and F. Xing, "Dynamic mechanical properties and microstructure of graphene oxide nanosheets reinforced cement composites," *Nanomaterials,* vol. 7, p. 12, 2017. https://doi.org/10.3390/nano7120407
[76] Q. Wang, J. Wang, C.-x. Lu, B.-w. Liu, K. Zhang and C.-z. Li, "Influence of graphene oxide additions on the microstructure and mechanical strength of cement," *New Carbon Materials,* vol. 30, no. 4, pp. 349-356, 2015. ISSN 1872-5805, https://doi.org/10.1016/S1872-5805(15)60194-9.
[77] Z. Pan, L. He, L. Qiu, A. H. Korayem, G. Li, J. W. Zhu, F. Collins, D. Li, W. H. Duan and M. C. Wang, "Mechanical properties and microstructure of a graphene oxide-cement composite," *Cement and Concrete Composites,* vol. 58, pp. 140-147, 2015. https://doi.org/10.1016/j.cemconcomp.2015.02.001
[78] H. Du and S. D. Pang, "Dispersion and stability of graphene nanoplatelet in water and its influence on cement composites," *Construction and Building Materials,* vol. 167, pp. 403-413, 2018. https://doi.org/10.1016/j.conbuildmat.2018.02.046
[79] K. Gong, Z. Pan, A. H. Korayem, L. Qiu, D. Li, F. Collins, C. M. Wang and W. H. Duan, "Reinforcing Effects of Graphene Oxide on Portland Cement Paste," *Journal of Materials in Civil Engineering,* vol. 27, no. 2, 2015. https://doi.org/10.1061/(asce)mt.1943-5533.0001125
[80] B. Wang, R. Jiang and Z. Wu, "Investigation of the mechanical properties and microstructure of graphene nanoplatelet-cement composite," *Nanomaterials,* vol. 6, no. 11, 2016. https://doi.org/10.3390/nano6110200
[81] B. Wang and B. Pang, "Mechanical property and toughening mechanism of water reducing agents modified graphene nanoplatelets reinforced cement composites," *Construction and Building Materials,* vol. 226, pp. 699-711, 2019. https://doi.org/10.1016/j.conbuildmat.2019.07.229
[82] M. Wang, R. Wang, H. Yao, S. Farhan, S. Zheng and C. Du, "Study on the three dimensional mechanism of graphene oxide nanosheets modified cement," *Construction Building Materials,* vol. 126, pp. 730-739, 2016.
[83] T. Qureshi and D. Panesar, "Nano reinforced cement paste composite with functionalized graphene and pristine graphene nanoplatelets," *Composites Part B: Engineering,* 2020. 108063.
[84] S. Sharma and N. Kothiyal, "Comparative effects of pristine and ball-milled graphene oxide on physico-chemical characteristics of cement mortar nanocomposites," *Construction Building Materials,* vol. 115, pp. 256-268, 2016.
[85] A. Niş, N. Özyurt, and T. Özturan, “Variation of Flexural Performance Parameters Depending on Specimen Size and Fiber Properties,” J. Mater. Civ. Eng., vol. 32, no. 4, p. 04020054, 2020, https://doi.org/10.1061/(asce)mt.1943-5533.0003105.
[86] K. Gong, Z. Pan, A. Korayem, L. Qiu, D. Li and F. Collins, "Reinforcing effects of graphene oxide on portland cement paste," *Journal of Materials in Civil Engineering,* vol. 27, 2015. A4014010.

[87] Z. Pan, L. He, L. Qiu, A. H. Korayem, G. Li, J. W. Zhu, F. Collins, D. Li, W. H. Duan and M. C. Wang, "Mechanical properties and microstructure of a graphene oxide–cement composite," *Cement and Concrete Composites,* vol. 58, pp. 140-147, 2015. https://doi.org/10.1016/j.cemconcomp.2015.02.001.

[88] S. Sharma and N. Kothiyal, " Influence of graphene oxide as dispersed phase in cement mortar matrix in defining the crystal patterns of cement hydrates and its effect on mechanical, microstructural and crystallization properties," *RSC Advance,* vol. 5, pp. 52642-52657, 2015.

[89] B. Wang, R. Jiang and Z. Wu, "Investigation of the mechanical properties and microstructure of graphene nanoplatelet-cement composite," *Nanomaterials,* vol. 6, no. 11, p. 200, 2016.

[90] C. Lin, W. Wei and Y. Hu, "Catalytic behavior of graphene oxide for cement hydration process," *The Journal of Physics and Chemistry of Solids,* vol. 89, pp. 128-33, 2016.

[91] T. Qureshi and D. Panesar, "Impact of graphene oxide and highly reduced graphene oxide on cement based composites," *Construction and Building Materials,* vol. 206, pp. 71-83, 2019.

[92] W. Long, T. Ye, Y. Gu, H. Li and F. Xing, "Inhibited effect of graphene oxide on calcium leaching of cement pastes," *Construction and Building Materials,* vol. 202, pp. 177-188, 2019

[93] R. JADHAV and N. C. DEBNATH, "Computation of X-ray powder diffractograms of cement components and its application to phase analysis and hydration performance of OPC cemen," Bulletin of Materials Science, vol. 34, p. 1137–1150, 2011. https://doi.org/10.1007/s12034-011-0134-0

[94] S. Mindess, J. Young and D. Darwin, Concrete, second ed., New Jersey: Pearson Education Inc., 2003.

[95] J. Lai and W. Sun, "Dynamic behaviour and visco-elastic damage model of ultrahigh performance cementitious composite," *Cement and Concrete Research,* vol. 39, no. 11, pp. 1044-1051, 2009.

[96] N. Tran, T. Tran and D. Kim, "; High rate response of ultra-high-performance fiber-reinforced concretes under direct tension,," *Cement and Concrete Research,* vol. 69, pp. 72-87, 2015.

[97] K. Wille, M. Xu, S. El-Tawil and A. Naaman, "Dynamic impact factors of strain hardening UHP-FRC under direct tensile loading at low strain rates," *Materials and Structures,* vol. 49, no. 4, pp. 1351-1365, 2016.

[98] D.Y. Yoo and N. Banthia, "Impact resistance of ultra-high-performance fiber-reinforced concrete with different steel fibers," in *9th RILEM International Symposium on Fiber Reinforced Concrete (BEFIB 2016)*, Pacific Gateway Hotel, Vancouver, BC, Canada, 2016.

[99] P. Sukontasukkul, P. Pongsopha, P. Chindaprasirt and S. Songpiriyakij, "Flexural performance and toughness of hybrid steel and polypropylene fibre reinforced geopolymer," *Construction and Building Materials,* vol. 161, pp. 37-44, 2018. https://doi.org/10.1016/j.conbuildmat.2017.11.122.

[100] D. Yoo, S. Kang and Y. Yoon, "Effect of fiber length and placement method on flexural behavior, tension-softening curve, and fiber distribution characteristics of UHPFRC," *Construction Building Materails,* vol. 64, pp. 67-81, 2014.

[101] D. Yoo, G. Zi, S. Kang and Y. Yoon, " Biaxial flexural behavior of ultra-highperformance fiber-reinforced concrete with different fiber lengths and placement methods," *Cement and Concrete Composites,* vol. 63, pp. 51-66, 2015

[102] J. Li, C. Wu and H. Hao, "Investigation of ultra-high performance concrete slab and normal strength concrete slab under contact explosion," *Engineering Structures,* vol. 102, pp. 395-408, 2015

[103] J. Li, C. Wu, H. Hao, Z. Wang and Y. Su, "Experimental investigation of ultra-high performance concrete slabs under contact explosions," *The International Journal of Impact Engineering,* vol. 93, pp. 62-75, 2016.

[104] H. Y. Grisaro, D. Benamou and A. Mitelman, "Field tests of fiber reinforced concrete slabs subjected to close-in and contact detonations of high explosives," *International Journal of*

Impact Engineering, vol. 162, 2022. 104136.
https://doi.org/10.1016/j.ijimpeng.2021.104136.

Figure
Click here to access/download;Figure;Figure.docx
Click here to view linked References

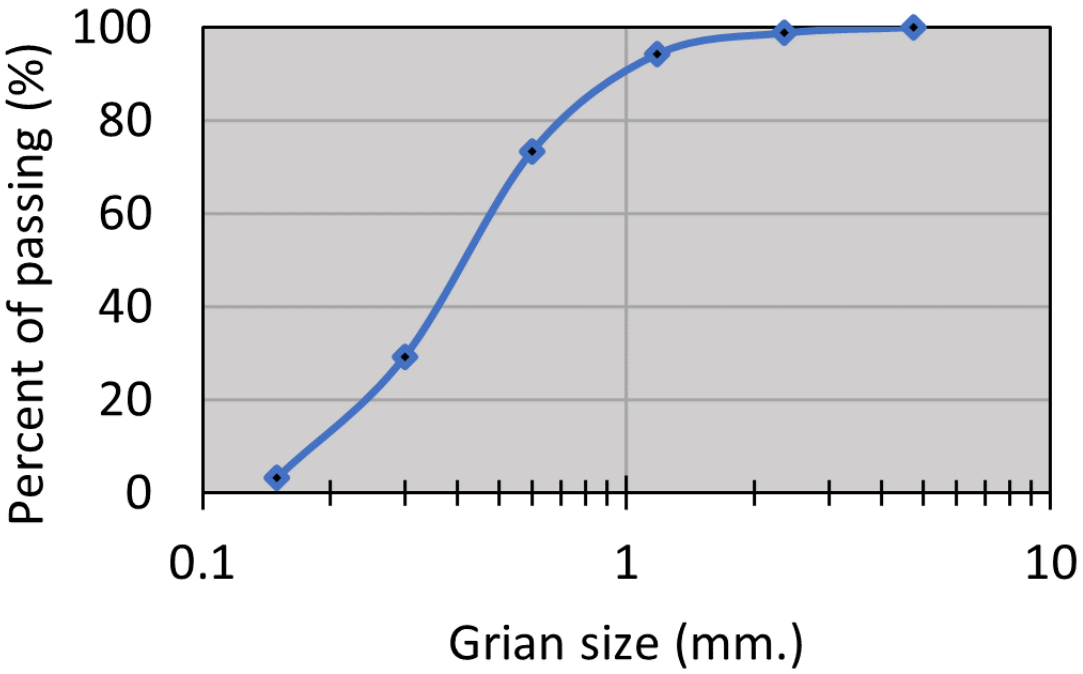

Figure 1. Grain size distribution of sand

Table 1. Properties of steel fiber

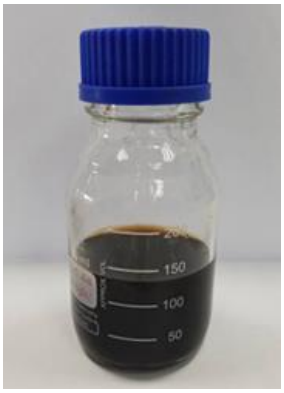

Table 2. GO solution properties

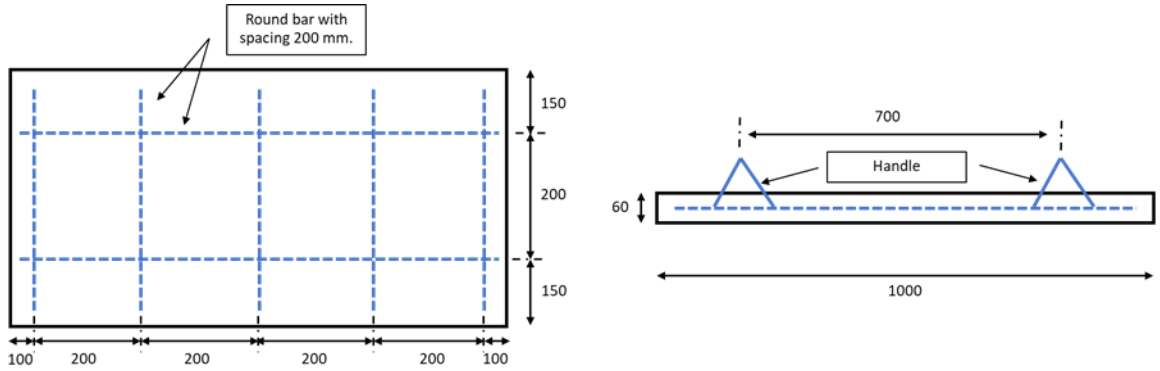

Figure 2. Steel reinforcement of specimen (unit in mm)

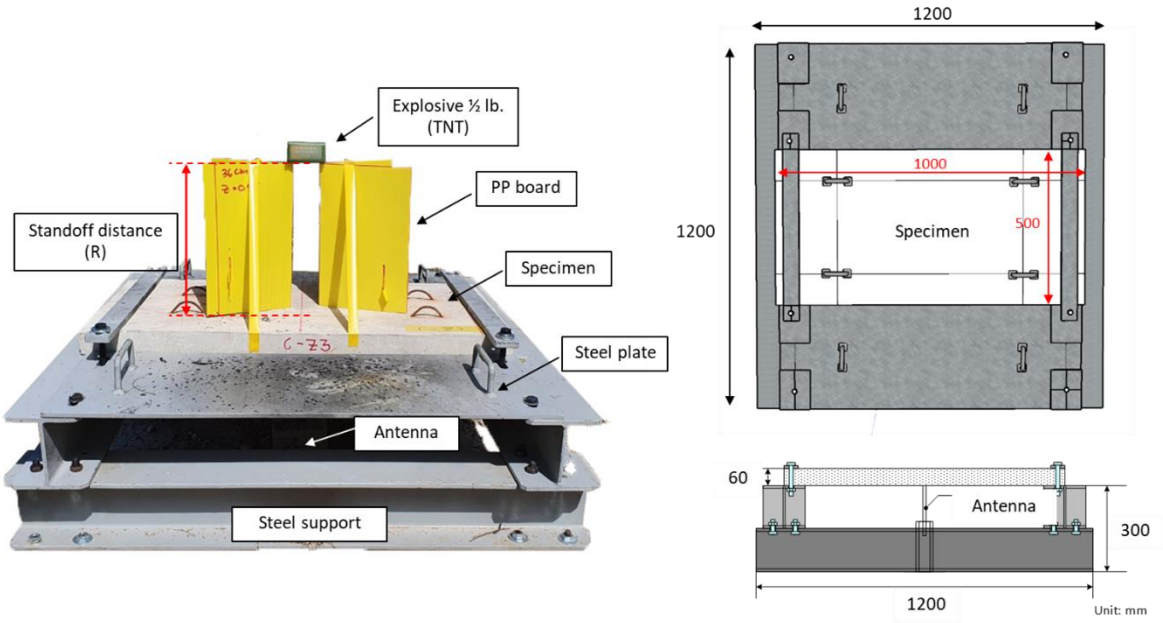

Figure 3. Blast impaction test setup (unit in mm)

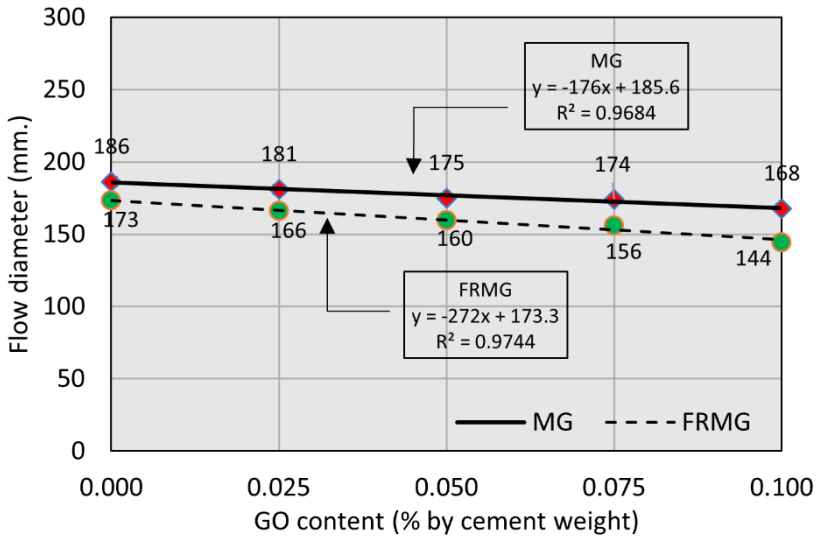

Figure 4. Flow diameter

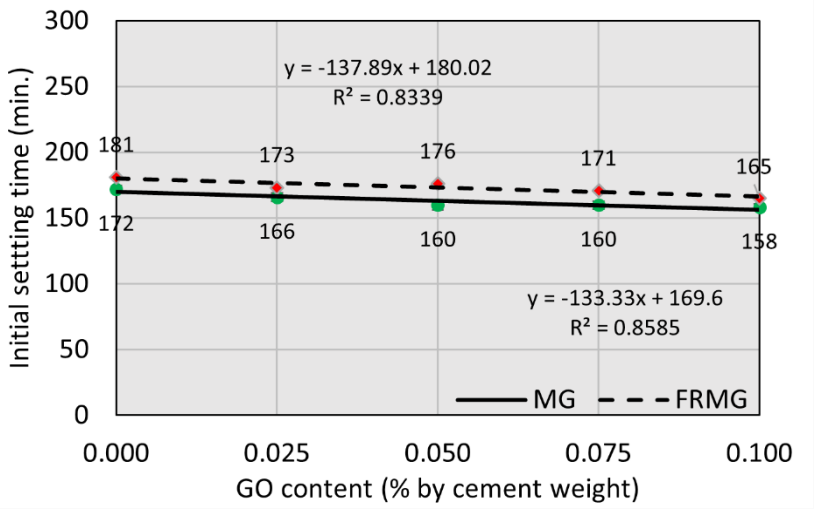

Figure 5a. Setting time

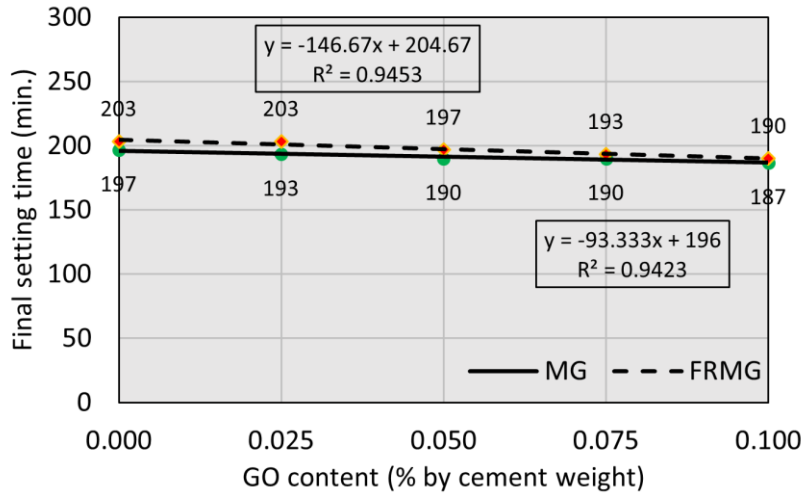

Figure 5b. Setting time

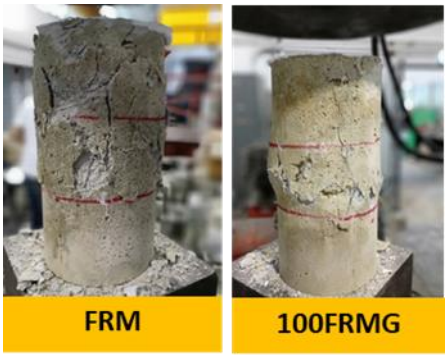

Figure 6a. Compression failure patterns: (a) brittle and (b) ductile modes

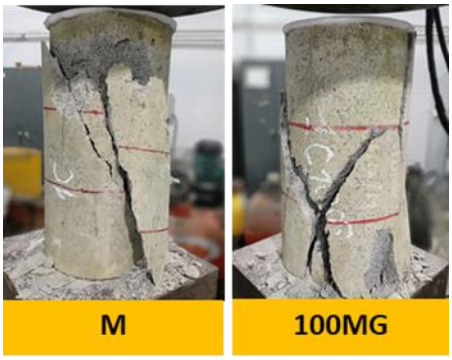

Figure 6b. Compression failure patterns: (a) brittle and (b) ductile modes

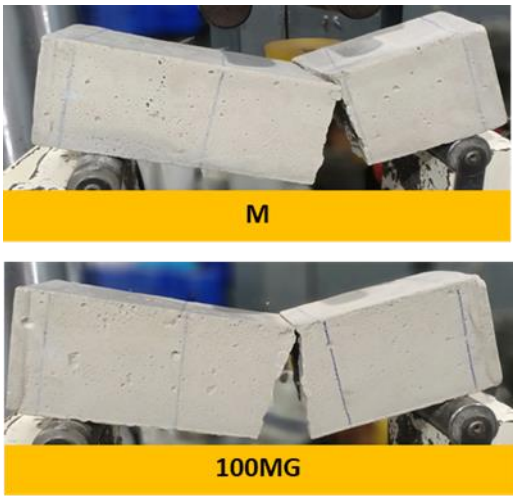

Figure 7a. Flexural failure patterns: (a) brittle and (b) ductile

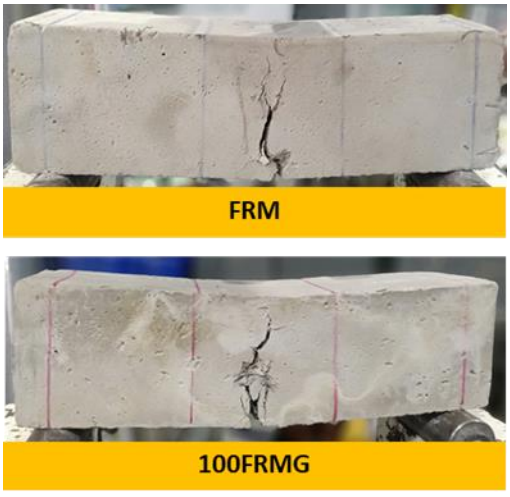

Figure b. Flexural failure patterns: (a) brittle and (b) ductile

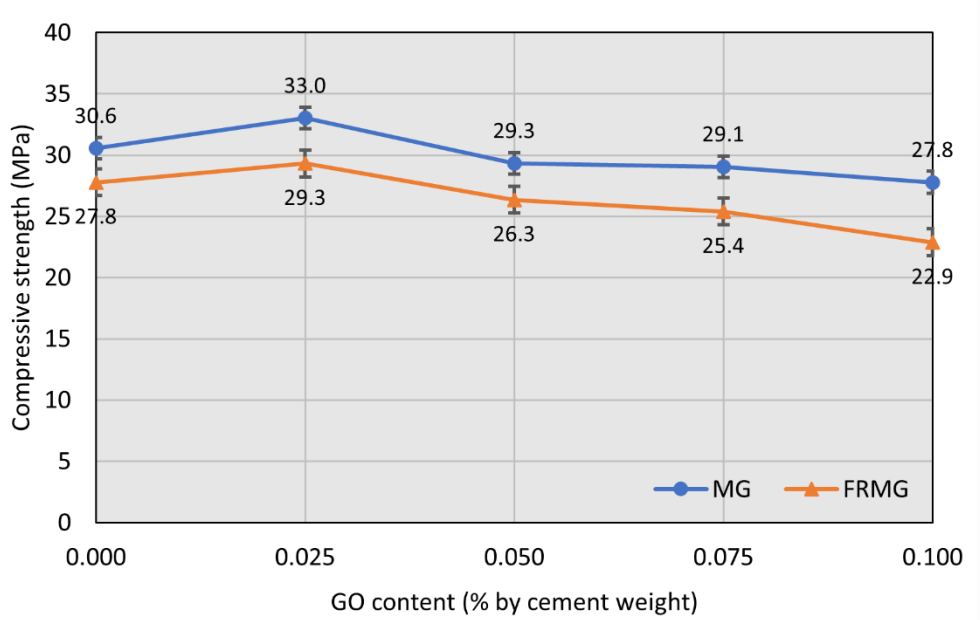

Figure 8. Compressive strength

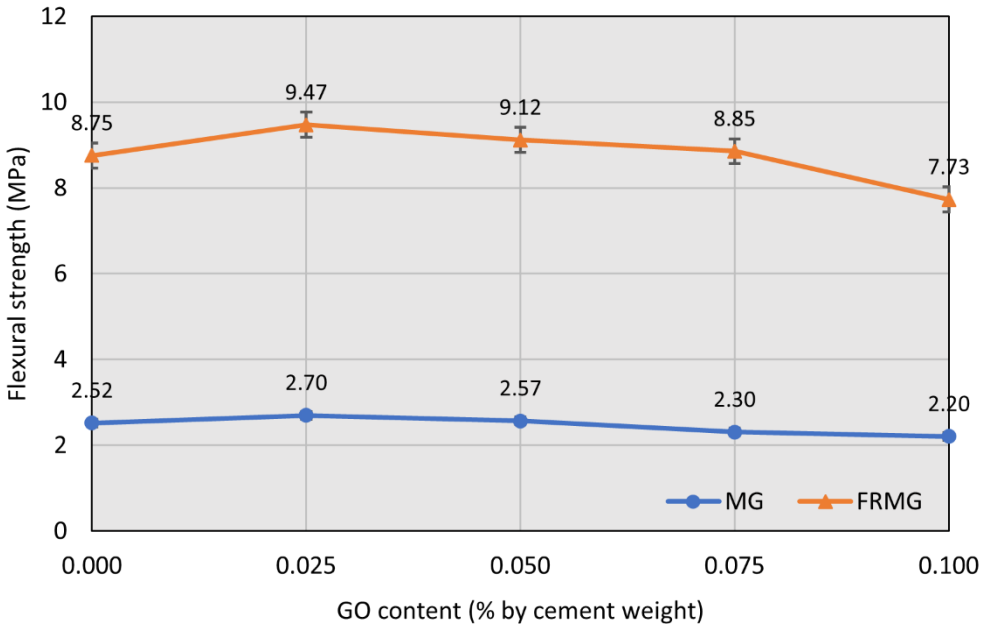

Figure 9. Flexural strength

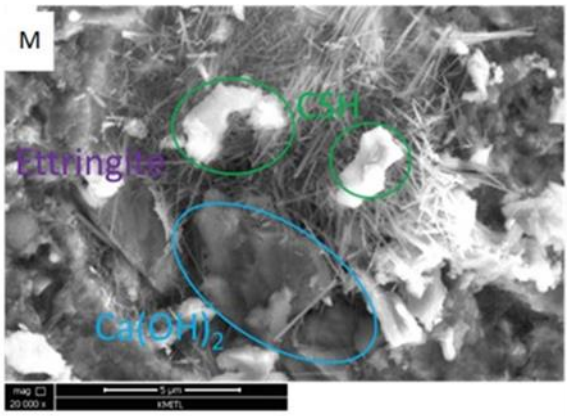

Figure 10a. The SEM of mortar mixed with graphene oxide (a) M, (b) 25MG, (c) 75MG, (d) 100MG

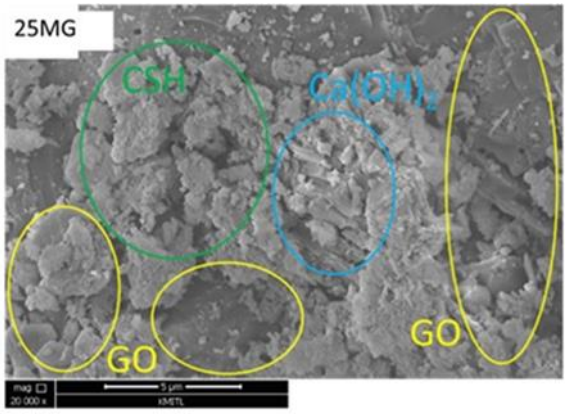

Figure 10b. The SEM of mortar mixed with graphene oxide (a) M, (b) 25MG, (c) 75MG, (d) 100MG

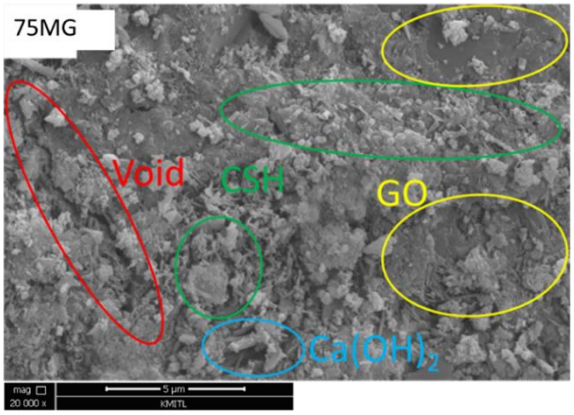

Figure 10c. The SEM of mortar mixed with graphene oxide (a) M, (b) 25MG, (c) 75MG, (d) 100MG

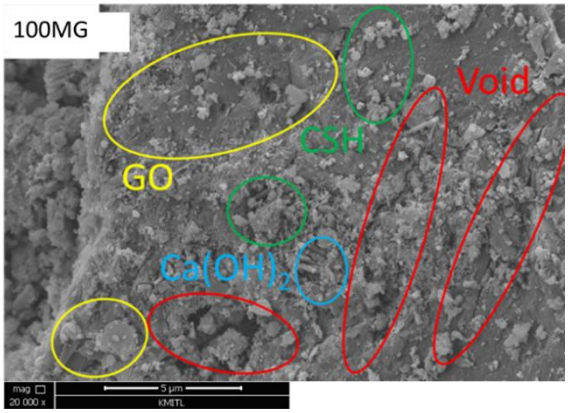

Figure 10d. The SEM of mortar mixed with graphene oxide (a) M, (b) 25MG, (c) 75MG, (d) 100MG

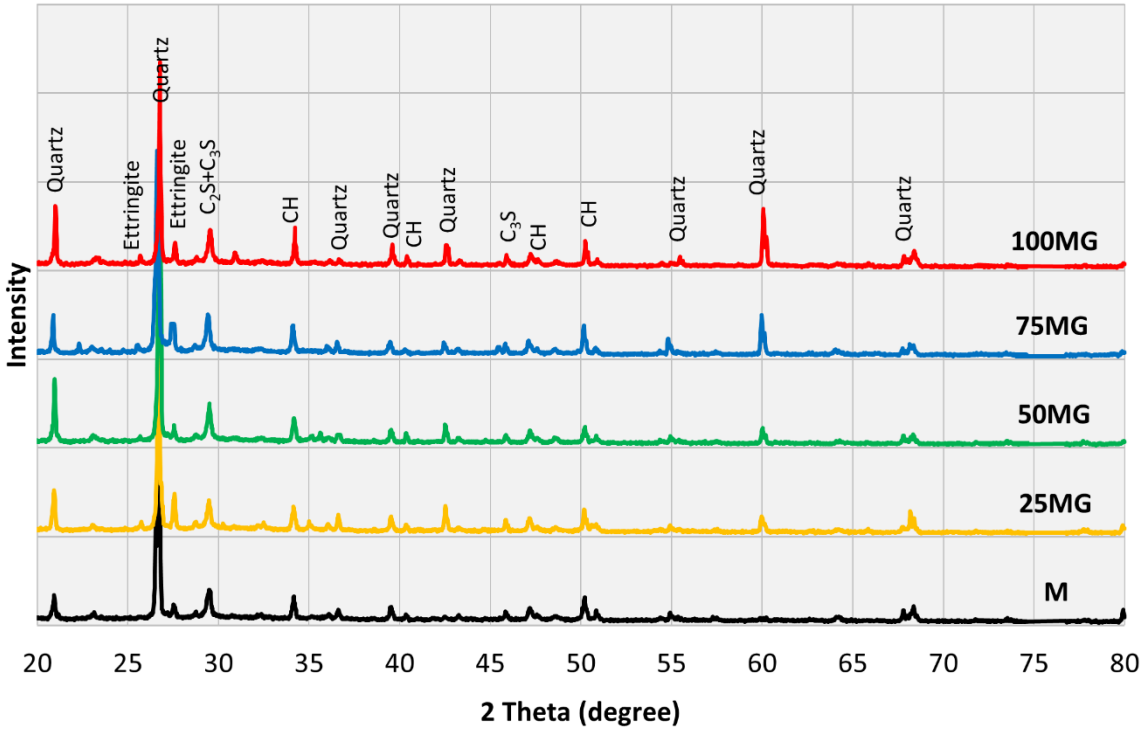

Figure 11. XRD pattern of MG

Figure 12a. Complete flexural failure pattern

Figure 12b. Complete flexural failure pattern

Figure 12c. Complete flexural failure pattern

Figure 13a. Flexural cracking pattern

Figure 13b. Flexural cracking pattern

Figure 13c. Flexural cracking pattern

Figure 14a. No major damage with microcracking pattern

Figure 14b. No major damage with microcracking pattern

Figure 14c. No major damage with microcracking pattern

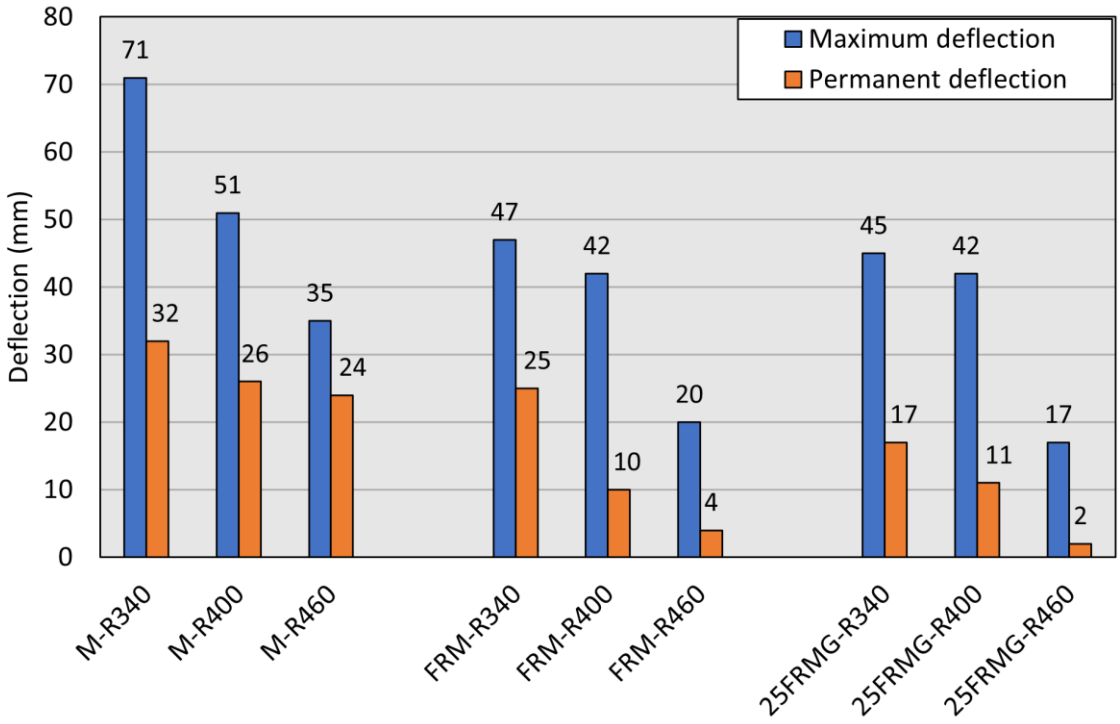

Figure 15. Deflection

Reviewer#1

No.	Reviewer's comments	Author response
1.	This short study is not recommended for publication in CBM	The authors would like to thank the reviewers for spending their time and effort to review this manuscript.
2.	Introduction does not cover important aspects of the GO use in concrete and fibre-reinforced concretes.	Thank you for the comment. Based on our literature review search, currently, there are about 14 articles covering several aspects on the application of GO in concrete. Also, only about 3 studies have been investigated on the effect of GO in concrete under impact loading, and none is on actual blast loading. Therefore, the objective of this study aims to fill the gap in the effect of GO to enhance FRC under actual blast loading.
3.	Methodology is short and insufficient.	Blast loading is considered one of a very difficult and costly tests to carry out. It is extremely dangerous and most likely to damage any instruments attached to the specimen. Many of blast loading tests often report damage patterns or measuring damage diameter or weight after the test. In our study, in addition to the failure mode, by carefully controlling the weight of TNT, an instrument to measure the deflection was equipped under the specimen which add more information to our study.
4.	No.of mixes are insufficient to comprehensively investigate the role of GO and steel fiber towards blast resistance.	Thank you for your comment, we would like to explain as follow. The use of TNT in Thailand requirement a permission from the army, in our study only limiting amount of TNT is permitted. This is therefore limited the number of our test. Also, due to the high expenses and high risks related to blasting test, the number of test samples is limited to the mix proportion that pass the required properties from the static test.
5.	Complete load vs deflection behavior is missing to analyse the ductility of proposed or designed mixes.	Thank you for your comment. As mentioned in 3, there quite difficult to obtain load vs time from the blasting test. We can only calculate the pressure acting on the specimen from weight of TNT and distance.
6.	All results and discussion are not suitable for a length article publication.	Thank you for the comment, we have revised the article based on other reviewer's comments. Hopefully, it will meet your length requirement. Please kindly give us an opportunity to be reconsidered.

7.	Some conclusions are already drawn by previous studies, Focus should be on the novel/unique or key findings of present research.	We have improved the conclusion to focus on key findings in the revised manuscript.

Reviewer#2

No.	Reviewer's comments	Author response
1.	Abstract should be improved. The important research results should be provided in Abstract.	The abstract is revised as you suggested.
2.	In sec. 4.1.1, It is stated the reduction in workability, uniform dispersion and setting time is due to high specific surface area, So it is necessary to express the amount of specific surface area of GO in a table showing the physical properties of GO.	The specific surface area of GO of 100-200 m^2/g has been added to table 2 as suggested by the reviewer.
3.	In sec. 2.1, It is important for the reader to know what is the density of GO, so its inclusion in the above Table seems necessary. The physical properties table should include diameter, density, specific surface area, ...etc.	More information of GO properties have been added to Table 2 as suggested by the reviewer.
4.	In p.5 sec. 2.2, What standard has been used for sand? what is the lower and upper limits granulation for sand?	The standard for classifying granulation of sand is ASTM D 2487. "Sand" is the material passing a 4.75-mm sieve (No. 4) and retained on a 0.075-mm (No. 200) sieve. For more information, the grain size distribution of sand is added to Figure 1 in the manuscript.
5.	In p.9, line 1, separate the term "MGwhich".	Corrected as suggested by the reviewer.
6.	In p. 12 line 14, replace the word "cement" with the "mortar" in the following sentence. ..... there was no spalling of "cement" fragments found.....	Corrected as suggested by the reviewer.
7.	In p. 15 line 6, add "to" before the "Lt. Col. Amornthep somrat"	Corrected as suggested by the reviewer.

Reviewer#3

No.	Reviewer's comments	Author response
1.	In Page 2, Line 33-35. 'The optimum GO content giving the highest compressive and flexural strengths was determined and chosen to continue on to the blast loading tests.' This sentence is not clear. Please rewrite the sentence	The sentence was rewritten as follow: A series of experiments were carried out consisting of 2 stages: Stage 1) workability, setting time, compressive and flexural strength, and microstructure using SEM and XRD processes, and Stage 2) blasting loading test. The optimum GO dosage giving the highest compressive and flexural strengths from the 1^{st} stage was determined and chosen to continue on the 2^{nd} stage (blast loading test).

2.	Page 3 Lines 7-14. 'In the case of impact loading, FRC material has proven to be superior to plain concrete'. Please give the enhancement ratio for the impact resistance and energy. The below studies gives the ratio for the enhancements for the FRC in impact performance. -Effects of recycled tyre rubber and steel fibre on the impact resistance of slag-based self-compacting alkali-activated concrete -Effects of nanosilica and steel fibers on the impact resistance of slag based self-compacting alkali-activated concrete	Thank for your recommendation the following sentences were added to the introduction part. Niş et al. [24-25] indicated that the addition of short and long steel fibers at 1% by volume fraction enhanced the impact energy absorption of concrete by 20.5 and 64 times, respectively.
3.	Page 3 Lines 18-26. Please add nanosilica material to give examples for the concrete performance enhancements. Nanosilica is the one of the most used nanomaterial for the concrete production. Nanosilica improves durability resistance (a), bond strength (b), and fresh and hardened state performance (c). a- Effect of nano-silica on the chemical durability and mechanical performance of fly ash based geopolymer concrete b- Development of fly ash/slag based self-compacting geopolymer concrete using nano-silica and steel fiber c-Fresh and hardened state performance of self-compacting slag based alkali activated concrete using nanosilica and steel fiber	Thank you for your recommendation, the recommended articles are referred in the manuscript. and nano-silica to improve durability [49], bond strength [50], and mechanical performance [51].
4.	In Table 3, why the OPC amount was selected so high as 580 kg/m3? If the 340 or 400 kg/m3 binder content was utilized, which results will be influenced? Please explain.	The cement content was selected based on the required compressive strength. Since the target compressive strength of plain mortar was set at 30 MPa, the cement content was selected at 580 kg/m^3. As for your question, if the amount of cement is reduced to 340-400 kg/m^3 , which results will be influenced. In term of mechanical performance, the reduction of cement content could cause the compressive and flexural strengths to decrease. Subsequently, this will also lead to the reduction in the performance of FRC under blast loading test.
5.	Page 6. ''The rate of loading for the flexural test was set at 0.05 mm/min with a third-point loading pattern.'' The loading type is displacement-controlled? Why the notched beams are not utilized for the flexural strength?	In our study, the flexural test was performed in according to ASTM C1609 Flexural Testing of Fiber-Reinforced Concrete Beams which is a common test to access the performance of FRC under flexural load. It is capable of determining flexural strength, toughness,

		and residual strength. The standard does not require to test on a notched beam.
6.	In Figs. 3 and 4., flow diameter and setting time for the non-fibrous mixes were given. Please add the results of mixes including 2% steel fibers.	We have added the results on flow diameter and setting time for FRM in Figures 4 and 5.
7.	In Page 7, 'The addition of high specific surface area materials like GO also caused difficulty in achieving a uniform dispersion in the cement matrix'. When both 2% steel fibers and GO materials were included, how the uniform dispersion of the fibers controlled? Please explain.	The uniform distribution is performed by increasing mixing time and dividing fibers into small portions as follow: The specimen preparation process began with dry mixing cement and sand for 2 minutes. The liquid part (clean water and GO solution) was mixed together prior to adding to the dry mix. For uniformly dispersed GO, the mixing time was continued for about 3 minutes for all specimen types until the GO was fully dispersed in the fresh mortar. In cases of FRM, the steel fiber was added to the fresh mortar by dividing the fibers into 3 parts. Each part of fiber was distributed to the mixer and mixed continuously for 1 min. The fresh mortar was then cast into steel molds by dividing into 3 layers, compacted on a vibration table for 1 minute, and wrapped in plastic sheeting overnight. After 24 hours, the specimens were demolded and cured under water for 28 days.
8.	In Page 8, 'For both loading types, the optimum GO content was observed to be 0.025%.' What can be reason the reduction in the mechanical strengths for the higher usage like 0.1%? If the reason is the difficulty in mixing and good compaction, why superplasticizer is not utilized?	Thank you for the comment, in our study, we didn't use superplasticizer because the content of superplasticizer will have to be varied in wide ranges and it might provide undesired effects to the properties of MG and FRMG. However, there are some studies where superplasticizer was used and still, the compressive and tensile strengths was found to decrease at GP content of 0.1%, S. Sharma et al. [1] reported that the compressive and tensile strength decreased with an increasing GP content to 0.1% with the increasing dosage of superplasticizer. They are giving the reason that "the high concentration of GO is difficult to disperse and does not produce C-H crystals at same rate as when present in dispersed state". [1] S. Sharma, D. Susan, N. C. Kothiyal, and R. Kaur, "Graphene oxide prepared from mechanically milled graphite: Effect on

		strength of novel fly-ash based cementitious matrix," Constr. Build. Mater., vol. 177, pp. 10–22, 2018, doi: 10.1016/j.conbuildmat.2018.05.051.
9.	In Page 9, 'This was because large numbers of fibers (at high content of 2%) lowered the workability which caused poor compaction and high porosity.' For the study, please add the workability results for the FRC mixes.	The workability results in term of flow diameter of FRC mixes were added in Figure 4 as suggested by the reviewer.
10.	'In the case of flexural strength, the results were the opposite of the compressive strength. The flexural strength of FRM and FRMG was higher than that of M and MG regardless of the GO content. This was due to the effect of fiber alignment which were mostly parallel to the stress plane when subjected to flexural loading.' Please support the sentence literature findings about the influence of fiber orientation on the flexural strength. - Variation of flexural performance parameters depending on specimen size and fiber properties	The recommended article is added to the manuscript to support the finding as follow. Niş et al. **Error! Reference source not found.** reported similarly that the fibers were more aligned and oriented along the casting direction in the specimens with thinner sections than the specimens with deep sections.
11.	In Figure 12, from side view (c), there are some visible cracks formed at the outside the blast region. Please mention about this.	We have mentioned this in the revised manuscript.
12.	In Fig. 13, bottom view, there are visible cracks also formed at bottom of the specimens. Especially, three big cracks are localized at the bottom releasing the stress where high tensile stresses are available. Please explain this clearly since no damage is written below the Figures.	The small cracks were mentioned in the revised manuscript. Since the cracks are quite small (as compared to the first 2 modes), they only occurred at the surface and did not propagate through the thickness (no visible crack along the thickness from the side view of Figure 14), we would like to call them 'microcrack'. At the bottom surface, small microcracks were visually observed. Since there is no evidence of cracks at the side view photo (Figure 14), this indicated that these cracks only occurred at the surface but did not propagate through the thickness.
13.	'However, in the case of permanent deflection, 25FRMG exhibited lower permanent deflection than FRM. This is perhaps due to the flexibility of GO which allowed the panels to rebound back more effectively, resulting in less permanent deflection.' Another reason can be the enhanced bond strength of specimens with	Revised as suggested by the reviewer. This is perhaps due to the flexibility of GO and the enhanced bond strength between steel fibers and GO material which allowed the panels to rebound back more effectively and limited the deflection of the specimen, resulting in less permanent deflection[46].

	steel fibers and GO material, limiting the deflection of the specimens.	
14.	In conclusion, please remove ' *blast resistance'	Corrected as suggested by the reviewer.
15.	In conclusion, 'no damage' may be changed as less damage due to the existence of flexural cracks at bottom portion.	Changed the word “no damage” to “no major damage with microcracking”.
16.	Before the conclusion points, please give the short summary of the study and explain what is GO used in the study.	Revised as suggested by the reviewer.

Click here to view linked References

Highlights

- Workability and setting time decreased with the increasing graphene oxide content.
- The optimum graphene oxide content was observed at 0.025% by cement weight.
- The decrease in voids was observed in mortar incorporating GO.
- GO enhanced blast resistance of FRM as seen by less damage and less permanent deflection.

Click here to view linked References

Credit author statement

Sittisak Jamnam: Conceptualization, Methodology**,** Investigate. **Buchit Maho:** Conceptualization, Methodology, Investigate, Writing – review & editing. **Apisit Techphatthanakon**: Methodology, Investigate. **Chesta Ruttanapun**: Resources support. **Peerasak Aemlaor:** Investigate, Formal analysis. **Hexin Zhang**: Supervision, Writing – review & editing. **Piti Sukontasukkul:** Supervision, Conceptualization, Writing – review & editing.

Title page Click here to view linked References

Effect of Graphene Oxide Nanoparticles on Blast Load Resistance of Steel Fiber Reinforced Concrete

Sittisak Jamnam[a], Buchit Maho[b*], Apisit Techaphatthanakon[a], Chesta Ruttanapun[c], Peerasak Aemlaor[d], Hexin Zhang[e], Piti Sukontasukkul[a],

[a] *Construction and Building Materials Research Center, Department of Civil Engineering, King Mongkut's University of Technology North Bangkok, Bangkok, Thailand*
[b] *Department of Civil Engineering, Faculty of Engineering, Rajamangala University of Technology Phra Nakhon, Bangkok, Thailand*
[c] *Smart Materials Research and Innovation Unit (SMRIU), Faculty of Science, King Mongkut's Institute of Technology Ladkrabang, Chalongkrung Road, Ladkrabang, Bangkok, Thailand*
[d] *Education Division, Chulachomklao Royal Military Academy, Thailand*
[e] *School of Engineering and the Built Environment, Edinburgh Napier University, Edinburgh, Scotland, United Kingdom*

Corresponding author: buchit.m@rmutp.ac.th

Acknowledgements

The authors would like to dedicate this work to Lt. Col. Amornthep Somrat for his strong devotion to this research, he will always be in our memories.

The research was funded by the Armament Research Fellowship Program for Enhancement of Armed Forces and National Defense Thailand. The authors would like to acknowledge support from Smart Materials Research and Innovation Unit, KMITL for providing the graphene oxide, Chulachomklao Royal Military Academy for supporting detonation, and also from King Mongkut's University of Technology North Bangkok and Rajamangala University of Technology Phra Nakhon for laboratory support. The last author would like to acknowledge funding from the National Science, Research and Innovation Fund (NSRF) and King Mongkut's University of Technology North Bangkok (KMUTNB) under the contract no. KMUTNB-FF-66-02. Special thank is also to Ruth Saint for proofreading the manuscript.

April 22, 2022

Professor Michael C. Forde
Chief Editor of Construction and Building Materials

Re: Conflict of interest

Dear Sir,

Regarding the submission of a manuscript on the title "Effect of Graphene Oxide Nanoparticles on Blast Load Resistance of Steel Fiber Reinforced Concrete" for your consideration to be published on your journal, the authors declare that they have no conflict of interest.

Please let me know should you require any further information. Look forward to hearing back from you.

Sincerely yours,

Buchit Maho, Ph.D.
Corresponding author

Department of Civil Engineering, Faculty of Engineering
Rajamangala University of Technology Phra Nakhon
1381 Pracharath I Road, Wong Sawang, Bangsue,
Bangkok 10800 Thailand
Tel : +66 (0) 2665-3777, +66 (0) 2665-3888
Fax : +66 (0) 2665-3758
Email : buchit.m@rmutp.ac.th

April 22, 2022

Professor Michael C. Forde
Chief Editor of Construction and Building Materials

Re: Conflict of interest

Dear Sir,

Regarding the submission of a manuscript on the title “Effect of Graphene Oxide Nanoparticles on Blast Load Resistance of Steel Fiber Reinforced Concrete” for your consideration to be published on your journal, the authors declare that they have no conflict of interest.

Please let me know should you require any further information. Look forward to hearing back from you.

Sincerely yours,

Buchit Maho, Ph.D.
Corresponding author

Department of Civil Engineering, Faculty of Engineering
Rajamangala University of Technology Phra Nakhon
1381 Pracharath I Road, Wong Sawang, Bangsue,
Bangkok 10800 Thailand
Tel : +66 (0) 2665-3777, +66 (0) 2665-3888
Fax : +66 (0) 2665-3758
Email : buchit.m@rmutp.ac.th